Dynamics and control of stochastically switching networks: beyond fast switching

Russell Jeter, Maurizio Porfiri, and Igor Belykh

Abstract Many complex systems throughout science and engineering display on-off intermittent coupling among their units. Stochastically blinking networks as a specific type of temporal networks are particularly relevant models for such sporadically interacting systems. In blinking networks, connections between oscillators stochastically switch in time with a given switching period. Most of the current understanding of dynamics of such switching temporal networks relies on the fast switching hypothesis, where the network dynamics evolves at a much faster time scale than the individual units. In this chapter, we go beyond fast switching and uncover highly nontrivial phenomena by which a network can switch between asynchronous regimes and synchronize against all odds. We review a series of our recent papers and provide analytical insight into the existence of windows of opportunity, where network synchronization may be induced through non-fast switching. Using stability and ergodic theories, we demonstrate the emergence of windows of opportunity and elucidate their nontrivial relationship with network dynamics under static coupling. In particular, we derive analytical criteria for the stability of synchronization for two coupled maps and the ability of a single map to control an arbitrary network of maps. This work not only presents new phenomena in stochastically switching dynamical networks, but also provides a rigorous basis for understanding the dynamic mechanisms underlying the emergence of windows of opportunity and leveraging non-fast switching in the design of temporal networks.

Russell Jeter
Department of Biomedical Informatics, Emory University, Atlanta, Georgia 30322, USA, e-mail: rjeter@emory.edu

Maurizio Porfiri
Department of Mechanical and Aerospace Engineering, New York University Tandon School of Engineering, Brooklyn, New York 11201, USA, e-mail: mporfiri@nyu.edu

Igor Belykh
Department of Mathematics and Statistics and Neuroscience Institute, Georgia State University, P.O. Box 4110, Atlanta, Georgia, 30302-410, USA, e-mail: ibelykh@gsu.edu

Key words: Blinking networks, Averaging, Master Stability Function, Stochastic Stability, Window of Opportunity

1 Introduction

Collective behavior within networks has received a considerable amount of attention in the literature, from animal grouping to robotic motion [77, 71]. One type of collective behavior, synchronization, is particularly important in how prevalent it is in real-world systems [10, 59, 3]. Synchronization is one of the most basic instances of collective behavior, and one of the easiest to diagnose: it occurs when all of the nodes in a network act in unison. Typically, it manifests in ways similar to a school of fish moving as one larger unit to confuse or escape from a predator [15], or a collection of neurons firing together during an epileptic seizure [53].

Significant attention has been devoted to the interplay between node dynamics and network topology which controls the stability of synchronization [57, 8, 46, 54]. Most studies have looked at networks whose connections are static; networks with a dynamically changing network topology, called temporal or evolving networks, are only recently appearing into the scientific literature [28, 20, 76, 38, 7, 30, 72, 47, 48, 51, 17, 80, 70, 69, 67, 63, 61, 60, 28, 20, 79, 21, 18, 74, 73, 31, 32, 5, 22, 27, 1, 24, 19, 49, 50] (see the recent books [36, 37] for additional references).

A particular class of evolving dynamical networks is represented by on-off switching networks, called "blinking" networks [7, 69] where connections switch on and off randomly and the switching time is fast, with respect to the characteristic time of the individual node dynamics. As summarized in a recent review [6], different aspects of synchronization, consensus, and multistability in stochastically blinking networks of continuous-time and discrete-time oscillators have been studied in the fast-switching limit where the dynamics of a stochastically switching network is close to the dynamics of a static network with averaged, time-independent connections. While a mathematically rigorous theory of synchronization in fast-switching blinking networks is available [7, 30, 72, 70, 69, 67, 63, 61, 60, 31, 32, 5, 40], the analysis of synchronization in non-fast switching networks of continuous-time oscillators has proven to be challenging and often elusive.

Non-fast switching connections yield a plethora of unexpected dynamical phenomena, including (i) the existence of a significant set of stochastic sequences and optimal frequencies for which the trajectory of a multistable switching oscillator can converge to a "wrong" ghost attractor [5] and (ii) bounded windows of intermediate switching frequencies ("windows of opportunity") in which synchronization becomes stable in a switching network over bounded intervals of the switching frequency, which may not include the fast switching limit [40]. As a result, networks that do not synchronize in the fast switching limit may synchronize for non-fast switching, and then lose synchronization as the frequency is further reduced. Found numerically in networks of continuous-time Rössler and Duffing oscillators [40] and Rosenzweig-MacArthur food chain models [41], the emergence of windows of op-

portunity calls for a rigorous explanation of unexpected synchronization from non-fast switching. Blinking networks of discrete-time systems (maps) with non-fast switching offer such a mathematical treatment [26, 62, 39, 42, 66]. More precisely, the switching period in discrete-time networks can be quantified as a number of the individual map's iterates such that rescaling of time yields a new, multi-iterate map that is more convenient to work with. This enables the formulation of a rigorous mathematical framework for the analysis of the stochastic stability of synchronization as a function of the switching period.

The purpose of this chapter is to give a detailed overview of this rigorous mathematical framework and reveal the central role of non-fast switching which may provide opportunity for stochastic synchronization in a range of switching periods where fast switching fails to synchronize the maps. We start with a historical perspective and a short review of the existing fast-switching theory for networks of continuous-time oscillators and discuss a motivating example of coupled Rössler oscillators with non-fast switching (Sec. 2). Then, we present the stochastic model of coupled maps and introduce the mean square stability of the transverse dynamics. To isolate the delicate mechanisms underpinning stochastic synchronization, we consider two coupled maps with independent identically distributed stochastic switching and study the stability of synchronization as a function of the switching period (Sec. 3). In Sec. 4, we extend our rigorous toolbox to assess the mean-square stability of controlled synchronization in broadcaster-network systems. We examine the feasibility of on-off broadcasting from a single reference node to induce synchronization in a target network with connections from the reference node that stochastically switch in time with an arbitrary switching period. Internal connections within the target network are static and promote the network's resilience to externally induced synchronization. Through rigorous mathematical analysis, we uncover a complex interplay between the network topology and the switching period of stochastic broadcasting, fostering or hindering synchronization to the reference node. With coupled chaotic tent maps as our test-bed, we prove the emergence of "windows of opportunity" where only non-fast switching periods are favorable for synchronization. The size of these windows of opportunity is shaped by the Laplacian spectrum such that the switching period needs to be manipulated accordingly to induce synchronization. Surprisingly, only the zero and the largest eigenvalues of the Laplacian matrix control these windows of opportunities for tent maps within a wide parameter region.

2 The Blinking Network Model: Continuous-Time Systems

"Blinking" networks were originally introduced for continuous-time oscillators in the context of network synchronization in [7]. A blinking network consists of N oscillators interconnected pairwise via a stochastic communication network:

$$\frac{d\mathbf{x}_i}{dt} = \mathbf{F}_i(\mathbf{x}_i) + \varepsilon \sum_{j=1}^{N} s_{ij}(t) P(\mathbf{x}_j - \mathbf{x}_i), \tag{1}$$

where $\mathbf{x}_i(t) \in \mathbb{R}^d$ is the state of oscillator i, $\mathbf{F}_i : \mathbb{R}^d \to \mathbb{R}^d$ describes the oscillators' individual dynamics, $\varepsilon > 0$ is the coupling strength. The $d \times d$ matrix P determines which variables couple the oscillators, $s_{ij}(t)$ are the elements of the time-varying connectivity (Laplacian) matrix $G(t)$. The existence of an edge from vertex i to vertex j is determined randomly and independently of other edges with probability $p \in [0,1]$. Expressed in words, every switch in the network is operated independently, according to a similar probability law, and each switch opens and closes in different time intervals independently. All possible edges $s_{ij} = s_{ji}$ are allowed to switch on and off so that the communication network $G(t)$ is constant during each time interval $[k\tau, (k+1)\tau)$ and represents an Erdős-Rényi graph of N vertices. Figure 1 gives an example of a "blinking" graph.

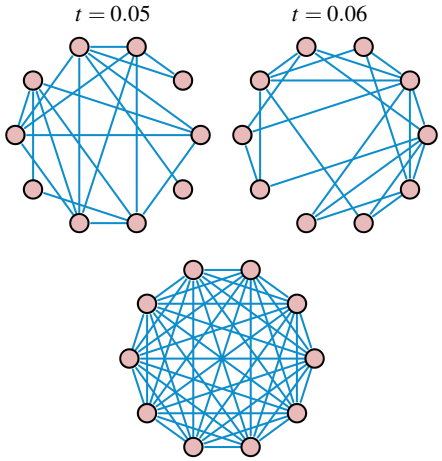

Fig. 1: (top). Two subsequent instances of the switching network. Probability of an edge $p = 0.5$, the switching time step $\tau = 0.01$. (Bottom). The corresponding averaged network where the switching connections of strength ε are replaced with static all-to-all connections of strength $p\varepsilon$, representing their mean value.

The switching network (1) is a relevant model for stochastically changing networks such as information processing cellular neural networks [30] or epidemiological networks [70, 24, 41]. For example, independent and identically distributed (i.i.d.) stochastic switching of packet networks communicating through the Internet comes from the fact that network links have to share the available communication time slots with many other packets belonging to other communication processes and the congestion of the links by the other packets can also occur independently.

As far as network synchronization is concerned, local computer clocks, that are required to be synchronized throughout the network, are a representative example. Clock synchronization is achieved by sending information about each computer's time as packets through the communication network [7]. The local clocks are typically implemented by an uncompensated quartz oscillator. As a result, the clocks can be unstable/inaccurate and need to receive synchronizing signals, that aim to reduce the timing errors. These signals must be sufficiently frequent to guarantee sufficient precision of synchronization between the clocks. At the same time, the communication network must not be overloaded by the administrative signals. This is a compromise between the precision of synchronization and the traffic load on the network. Remarkably, this blinking network administration can provide precise functioning of a network composing of imprecise elements. It also indicates the importance of optimal switching frequencies that ensure this compromise.

2.1 Historical Perspective: Fast Switching Theory

Over the years, various aspects of synchronization in fast switching networks of continuous-time oscillators have been extensively investigated [7, 72, 70, 69, 67, 63, 61, 40]. In particularly, it was rigorously proved in both continuous and discrete-time cases that if the switching frequency is sufficiently high, with respect to the characteristic time of the individual oscillators (fast switching limit), the stochastically blinking network can synchronize even if the network is disconnected at every instant of time.

Beyond synchronization, a rigorous theory for the behavior of stochastic switching networks of continuous-time oscillators in the fast switching limit was developed in [30, 31, 32, 5]. In general, it was proved in [31, 32] that for switching dynamical systems of this type, if the stochastic variables switch sufficiently fast, the behavior of the stochastic system will converge to the behavior of the averaged system in finite time, where the dynamical law is given by the expectation of the stochastic variables. These studies have also helped clarify a number of counterintuitive findings about the relationship between the stochastic network and its time-averaged counterpart. While intuition suggests that the switching network should follow the averaged system in the fast switching limit, this is not always the case, especially when the averaged system is multistable and its attractors are not invariant under the switching system. These attractors act as ghost attractors for the switching system, whereby the trajectory of the switching system can only reach a neighborhood of the ghost attractor, and remains close most of the time with high probability when switching is fast. In a multistable system, the trajectory may escape to another ghost attractor with low probability [32]. This theory uses the Lyapunov function method along with large deviation bounds to derive explicit conditions that connect the probability of converging towards an attractor of a multistable blinking network, the fast switching frequency, and the initial conditions. As the switching frequency decreases, it was shown that there is a range of "resonant" frequencies where the

trajectory of a multistable switching oscillator receives enough kicks in the wrong direction to escape from the ghost attractor against all odds [5].

Indeed, there are circumstances for which not converging to the averaged system is favorable, and the present fast-switching theory is not able to make definitive claims about the behavior of the stochastic system. This leads us to explore the effects of non-fast-switching on the dynamics of the switching network.

2.2 Beyond Fast Switching: A Motivating Example

We begin with a numerical example of the stochastic Erdős-Rényi network (1) composed of ten x-coupled Rössler oscillators:

$$\begin{cases} \dot{x}_i = -(y_i + z_i) + \varepsilon \sum_{j=1}^{10} s_{ij}(t)(x_j - x_i) \\ \dot{y}_i = x_i + a y_i \\ \dot{z}_i = b + z_i(x_i - c). \end{cases} \tag{2}$$

Hereafter, the intrinsic parameters are chosen and fixed as follows: $a = 0.2$, $b = 0.2$, $c = 7$. The averaged network is an all-to-all network with a fixed coupling strength $p\varepsilon$. Synchronization in a network of x-coupled Rössler systems is known [57] to destabilize after a critical coupling strength ε^*, which depends on the eigenvalues of the connectivity matrix G. We choose the coupling strengths in the stochastic network such that the coupling in the averaged network is defined by one of the three values, marked in Fig. 2. In particular, for $\varepsilon = 1$, synchronization in the averaged network is unstable. As a result, synchronization in the fast-switching network is also unstable. Surprisingly, there is a window of intermediate switching frequencies for which synchronization becomes stable (see Fig. 3). In fact, the stochastic network switches between topologies whose large proportion does not support synchronization or is simply disconnected.

To better isolate the above effect and gain insight into what happens when switching between a connected network in which the synchronous solution is unstable, and a completely disconnected network in which the nodes' trajectories behave independently of one another, we consider a two-node Rössler network (2). Figure 4 demonstrates the emergence of synchronization windows for various intermediate values of τ for which the fast-switching network does not support synchronization. In essence, the system is switching between two *unstable* systems, and yet when the switching period τ is in a favorable range within a window of opportunity, the system stabilizes.

Observed numerically in the network of continuous-time oscillators, this phenomenon calls for a more rigorous study to isolate the principal mechanisms underpinning unexpected synchronization from non-fast switching. The following sections aim at establishing such an analytical insight in more analytically tractable networks of discrete-time oscillators.

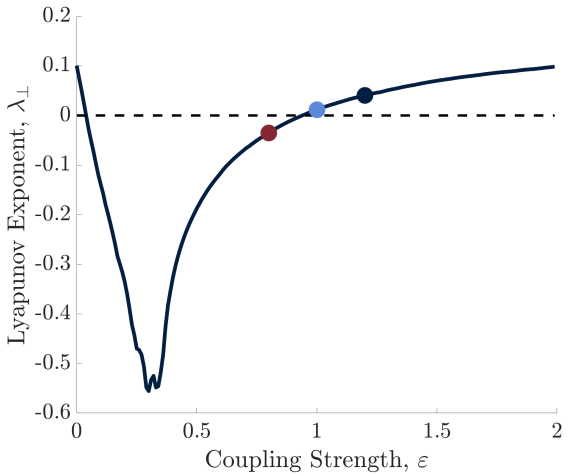

Fig. 2: Transversal stability of synchronization in the averaged ten-node x-coupled Rössler system, expressed via the largest transversal Lyapunov exponent. Synchronization is stable within the interval $\varepsilon^- < \varepsilon < \varepsilon^+$ [not shown]. The values of ε used in Fig. 3 are marked with dot in red, light blue, and navy.

3 Revealing Windows of Opportunity in Two Stochastically Coupled Maps

We focus on a *discrete-time* setting, where the coupling between the maps is held fixed for a finite number of time steps (switching period) and then it stochastically switches, independent of the time history. In this case, non-fast switching can be studied by re-scaling the time variable and consequently modifying the individual dynamics of the coupled maps. This enables the formulation of a rigorous mathematical framework for the analysis of the stochastic stability of synchronization as a function of the switching period. We restrict our analysis to two coupled maps with the two-fold aim of: i) providing a clear demonstration for the origin of this phenomenon, which may be hidden by topological factors in large networks and ii) establishing a toolbox of closed-form results for the emergence of windows of opportunity.

3.1 Network Model

We study the stochastic synchronization of two maps characterized by the state variables $x_i \in \mathbb{R}$, $i \in \{1,2\}$. We assume that the individual dynamics of each node evolves according to $x_i(k+1) = F(x_i(k))$, where $k \in \mathbb{Z}^+$ is the time step and

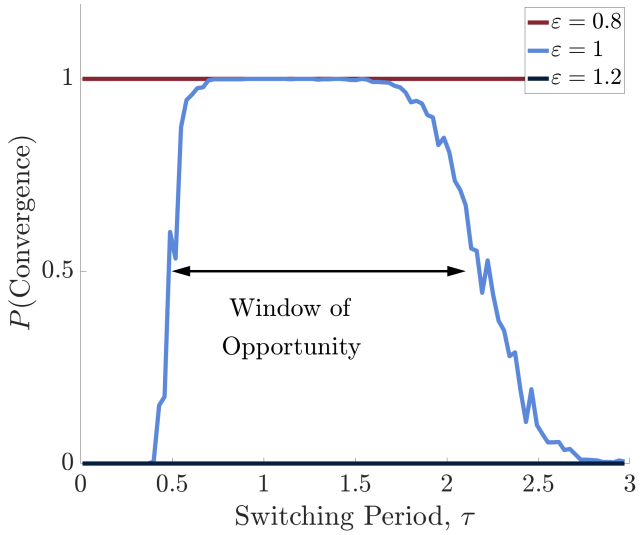

Fig. 3: Probability of synchronization in the ten-node stochastic Rössler network with differing coupling strengths, showing the effects of varying τ. These are coupling strengths for which synchronization in the averaged system is stable (red), weakly unstable (light blue), and strongly unstable (navy), respectively (cf. Fig. 2 for the values marked with appropriately colored dots). The bell-shaped curve corresponds to an optimal range of non-fast switching $0.6 < \tau < 2.2$ (the "window of opportunity"), where synchronization in the stochastic network becomes stable with high probability, whereas synchronization in the corresponding averaged system is unstable ($\varepsilon = 1$). Switching probability $p = 0.5$. Probability calculations are based on 1000 trials.

$F\colon \mathbb{R} \to \mathbb{R}$ is a smooth nonlinear scalar function. The maps are linearly coupled through the stochastic gains $\varepsilon_1(k), \varepsilon_2(k) \in \mathbb{R}$, such that

$$\begin{bmatrix} x_1(k+1) \\ x_2(k+1) \end{bmatrix} = \begin{bmatrix} F(x_1(k)) + \varepsilon_1(k)(x_2(k) - x_1(k)) \\ F(x_2(k)) + \varepsilon_2(k)(x_1(k) - x_2(k)) \end{bmatrix}. \tag{3}$$

Each of the sequences of coupling gains, $\varepsilon_1(0)$, $\varepsilon_1(1)$, $\varepsilon_1(2)$, … and $\varepsilon_2(0)$, $\varepsilon_2(1)$, $\varepsilon_2(2)$, …, is assumed to be switching stochastically with the same period $m \in \mathbb{Z}^+ \setminus \{0\}$. Every m time steps, the coupling gains simultaneously switch, such that $\varepsilon_1(mk) = \varepsilon_1(mk+1) = \ldots = \varepsilon_1(mk+m-1) = \tilde{\varepsilon}_1(k)$ and $\varepsilon_2(mk) = \varepsilon_2(mk+1) = \ldots = \varepsilon_2(mk+m-1) = \tilde{\varepsilon}_2(k)$ for every time step k, where $\tilde{\varepsilon}_1(0), \tilde{\varepsilon}_1(1), \ldots$ and $\tilde{\varepsilon}_2(0), \tilde{\varepsilon}_2(1), \ldots$ are two sequences of independent and identically distributed random variables.

The evolution of the coupled maps in equation (3) is determined by the random variables $\tilde{\varepsilon}_1$ and $\tilde{\varepsilon}_2$, from which the coupling gains are drawn. In general, these ran-

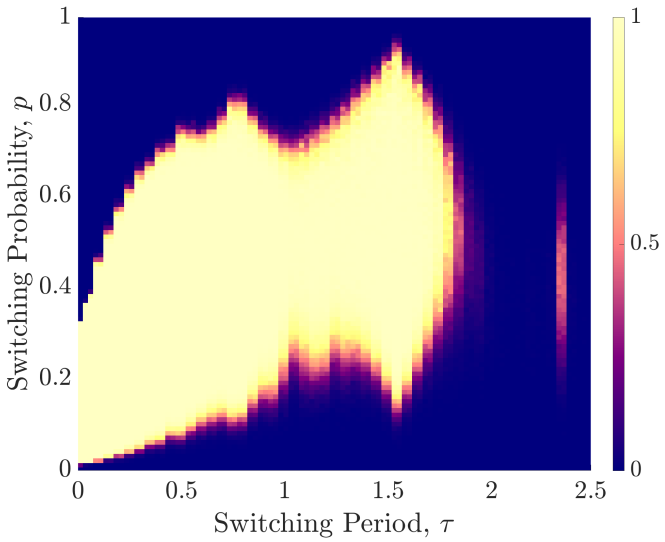

Fig. 4: Probability of synchronization in the two-node Rössler network (2) as a function of the switching probability p and switching period τ. Yellow (lighter) colors correspond to higher probability of convergence (with light yellow at probability 1) and blue (darker) colors correspond to lower probabilities (dark blue at probability 0). The coupling strength of the connection is fixed at $\varepsilon = 7$. As p increases, $p\varepsilon$, the effective coupling in the averaged/fast-switching network progresses through the window of synchrony indicated in Fig. 2. For the two-node network this interval is $p\varepsilon \in [0.08\ 2.2]$, yielding the stability range $p \in [0.011\ 0.31]$ (the yellow interval on the y-axis) for $\varepsilon = 7$ and small τ. Probability calculations are based on 1000 trials.

dom variables may be related to each other and may not share the same distribution. For example, in the case of uni-directional stochastic coupling, one of the random variables is zero; on the other hand, for bi-directional interactions, the two random variables coincide.

The majority of the work on stochastic synchronization of coupled discrete maps is largely limited to the case $m = 1$, for which the coupling gains switch at every time step [60]. In this case, the random variables $\varepsilon_i(0), \varepsilon_i(1), \varepsilon_i(2), \ldots$, for $i \in \{1,2\}$, are mutually independent. For each value of k, $x_1(k+1)$ and $x_2(k+1)$ are functions only of the previous values $x_1(k)$ and $x_2(k)$, and equation (3) reduces to a first order Markov chain with explicit dependence on time through the individual dynamics. In the case of $m > 1$, the random variables $\varepsilon_i(0), \varepsilon_i(1), \varepsilon_i(2), \ldots$, for $i \in \{1,2\}$, are no longer independent, which poses further technical challenges for the analysis of the system, while opening the door for rich behavior to emerge from the stochastically driven coupling.

The oscillators synchronize at time step k if their states are identical, that is, $x_1(k) = x_2(k)$. From equation (3), once the oscillators are synchronized at some time step, they will stay synchronized for each subsequent time step. The common synchronized trajectory $s(k)$ is a solution of the individual dynamics, whereby $s(k+1) = F(s(k))$. The linear stability of synchronization can be studied through the following variational equation, obtained by linearizing equation (3) in the neighborhood of the synchronization manifold:

$$\xi(k+1) = \left[F'(s(k)) - d(k)\right] \xi(k), \tag{4}$$

where prime indicates differentiation, $d(k) = \varepsilon_1(k) + \varepsilon_2(k)$ is the net coupling, and $\xi(k) = x_1(k) - x_2(k)$ is the synchronization error at time step k. Equation (4) defines the linear transverse dynamics of the coupled oscillators, measured with respect to the difference between their states $\xi(k)$. This quantity is zero when the two oscillators are synchronized. Equation (4) relies on the assumption that the mapping governing the individual dynamics, F, is differentiable everywhere. This assumption can be relaxed, however, to functions that are differentiable almost everywhere [58].

Only the sum of the two coupling gains $\varepsilon_1(k)$ and $\varepsilon_2(k)$ affects the transverse dynamics, thereby only the statistics of the random variable $d(k)$ modulate the linear stability of the synchronization manifold. To simplify the treatment of the variational problem in equation (4), we can rescale the time variable with respect to the switching period as follows:

$$\tilde{\xi}(k+1) = \prod_{i=0}^{m-1} (F'(s(mk+i)) - \tilde{d}(k))\tilde{\xi}(k), \tag{5}$$

where $\tilde{\xi}(k) = \xi(mk)$ and $\tilde{d}(k) = \tilde{\varepsilon}_1(k) + \tilde{\varepsilon}_2(k)$. Equation (5) casts the variational dynamics in the form of a first order time-dependent Markov chain, generated by a linear time-varying stochastic finite difference equation [23, 44].

It is important to emphasize that the synchronization manifold $x_1(k) = x_2(k)$ is an invariant set of the stochastic equation (3). Therefore, the dynamics of the synchronization manifold is governed by an attractor of the mapping function $F(s(k))$.

3.2 Mean Square Stability of Synchronization

In determining the stability of the synchronous state, various criteria can be considered, such as almost sure, in probability, and mean square [23, 44, 66]. The concept of mean square stability is particularly attractive, due to its practicality of implementation and its inclusiveness with respect to other criteria. Mean square stability of the synchronous state is ascertained through the analysis of the temporal evolution of the second moment of the error $\mathrm{E}[\tilde{\xi}^2]$, where $\mathrm{E}[\cdot]$ indicates expectation with respect to the σ-algebra generated by the switching. By taking the square of each side of equation (5) and computing the expectation, we obtain

$$\mathrm{E}\left[\tilde{\xi}^2(k+1)\right] = \mathrm{E}\left[\prod_{i=0}^{m-1}(F'(s(mk+i)) - \tilde{d}(k))^2\right]\mathrm{E}\left[\tilde{\xi}^2(k)\right]. \tag{6}$$

This recursion is a linear, time-varying, deterministic finite difference equation whose initial condition is $\tilde{\xi}^2(0)$, which is treated as a given value and not as a random variable. We say that equation (5) is mean square asymptotically stable if equation (6) is asymptotically stable, that is, if the Lyapunov exponent λ of equation (6) is negative. This implies that any small difference between the states of the oscillators will converge to zero in the mean square sense as time increases.

The Lyapunov exponent is a function of the switching period m and can be computed from equation (6) as follows [58]:

$$\lambda(m) = \lim_{k\to\infty}\frac{1}{k}\ln\prod_{j=0}^{k-1}\mathrm{E}\left[\prod_{i=0}^{m-1}(F'(s(mj+i)) - \tilde{d}(j))^2\right]. \tag{7}$$

In general, the stability of the synchronization manifold depends on the underlying synchronous solution, whereby $\lambda(m)$ in equation (7) explicitly depends on $s(k)$. In what follows, we focus on the case where $s(k)$ is a chaotic trajectory. We comment that our approach is based on the linearized dynamics in equation (4), which describes small perturbations from the synchronous state. Thus, our analysis is only applicable to the study of local stability of the synchronization manifold, and initial conditions cannot be arbitrarily selected in the basin of attraction.

3.3 Preliminary Claims

We assume that $\tilde{d}(k)$ takes values on a finite sample space $D = \{d_1, d_2, \ldots, d_n\}$ of cardinality n. For $l = 1, \ldots, n$, the probability that the net coupling is equal to d_l is chosen to be equal to p_l. For example, in the case of simple on-off connections, the individual coupling gains take values 0 and ε with corresponding probabilities p and $1-p$. Therefore, the net coupling gain $\tilde{d}(k)$ takes values $d_1 = 0, d_2 = \varepsilon$, and $d_3 = 2\varepsilon$ with corresponding probabilities $p_1 = p^2, p_2 = 2p(1-p)$ and $p_3 = (1-p)^2$.

From the individual values of the net coupling and their probabilities, we can evaluate the Lyapunov exponent in equation (7) as

$$\lambda(m) = \lim_{k\to\infty}\frac{1}{k}\sum_{j=0}^{k-1}\ln\left[\sum_{l=1}^{n} p_l \prod_{i=0}^{m-1}(F'(s(mj+i)) - d_l)^2\right]. \tag{8}$$

One of the central objectives of this study is to understand the relationship between the synchronizability of the coupled maps when statically coupled through the net coupling gains in D and their stochastic synchronizability when the net coupling randomly switches at a period m. Toward this aim, we adjust equation (8) to the case of statically coupled maps with a net coupling $d^\star$

$$\lambda^{\mathrm{st}}(d^\star) = \lim_{k\to\infty} \frac{1}{k} \sum_{j=0}^{k-1} \ln\left[(F'(s(j)) - d^\star)^2\right]. \tag{9}$$

For convenience, we write $\lambda_l^{\mathrm{st}} = \lambda^{\mathrm{st}}(d_l)$ for $l = 1,\ldots,n$. Depending on the value of d_l, the statically coupled systems may synchronize or not, that is, the corresponding error dynamics may be asymptotically stable or unstable.

If all of the Lyapunov exponents of the statically coupled systems are finite, then we can establish the following relationship between the Lyapunov exponent of the stochastic error dynamics (8) and $\{\lambda_r^{\mathrm{st}}\}_{r=1}^n$:

$$\lambda(m) = m\lambda_r^{\mathrm{st}} + \lim_{k\to\infty} \frac{1}{k} \sum_{j=0}^{k-1} \ln\left[\frac{\sum_{l=1}^n p_l \prod_{i=0}^{m-1}(F'(s(mj+i)) - d_l)^2}{\prod_{i=0}^{m-1}(F'(s(mj+i)) - d_r)^2}\right]. \tag{10}$$

Equation (10) is derived from equation (8) by: i) dividing and multiplying the argument of the logarithm by $\prod_{i=0}^{m-1}(F'(s(mj+i)) - d_r)^2$; ii) using the product rule of logarithms; and iii) applying equation (9) upon rescaling of the time variable by the period m.

By multiplying both sides of equation (10) by p_r and summing over r, we obtain the following compact relationship between the Lyapunov exponent of the stochastic dynamics and the individual Lyapunov exponents for statically coupled maps:

$$\lambda(m) = m\sum_{l=1}^n p_l \lambda_l^{\mathrm{st}} + \lim_{k\to\infty} \frac{1}{k} \sum_{j=0}^{k-1} \ln \frac{\sum_{l=1}^n p_l \zeta_l(j)}{\prod_{l=1}^n \zeta_l^{p_l}(j)}. \tag{11}$$

Here, we have introduced:

$$\zeta_l(j) = \prod_{i=0}^{m-1} (F'(s(mj+i)) - d_l)^2, \tag{12}$$

which we assume to be different than zero to ensure that the Lyapunov exponent stays finite.

The first summand on the right-hand side of equation (11) is linearly proportional to the switching period m and the "effective" Lyapunov exponent $\bar{\lambda} = \sum_{l=1}^n p_l \lambda_l^{\mathrm{st}}$, which corresponds to the average of the Lyapunov exponents associated with the statically coupled maps, weighted by the probability of the corresponding switching. The second summand is a residual quantity, which is always nonnegative and encapsulates the complex dependence of the transverse dynamics on the switching period beyond the linear dependence associated with the first summand.

3.4 Necessary Condition for Mean Square Synchronization

Proposition 3.1. *The synchronization of the stochastic system (3) is mean square stable only if the effective Lyapunov exponent $\bar{\lambda}$ is negative.*

Proof. A lower bound for the Lyapunov exponent $\lambda(m)$ can be obtained by applying the weighted arithmetic-geometric mean inequality [13]

$$\prod_{l=1}^{n} \zeta_l^{p_l} \leqslant \sum_{l=1}^{n} p_l \zeta_l. \tag{13}$$

From inequality (13), it follows that the argument of the logarithm in equation (11) is larger than or equal to 1. As a result, we obtain

$$\lambda(m) \geqslant m\bar{\lambda}. \tag{14}$$

This inequality establishes that for $\lambda(m)$ to be negative, $\bar{\lambda}$ must also be negative. □

Remark 1. From the previous claim, we posit if none of the Lyapunov exponents $\{\lambda_r^{\mathrm{st}}\}_{r=1}^n$ are negative, synchronization is not feasible for any selection of m and $\{p_r\}_{r=1}^n$. Thus, stochastic synchronization cannot be achieved without at least one coupling configuration to support synchronization. This is in contrast with observations from continuous-time systems which indicate the possibility of stable synchronization even if none of the coupling configurations support synchronization [40, 41].

Remark 2. The weighted arithmetic and geometric mean, introduced in (13), are equal if and only if $\zeta_1 = \zeta_2 = \ldots = \zeta_n$. Thus, inequality (14) reduces to an equality if and only if

$$\prod_{i=0}^{m-1} (F'(s(mj+i)) - d_1)^2 = \prod_{i=0}^{m-1} (F'(s(mj+i)) - d_2)^2 = \\ \ldots = \prod_{i=0}^{m-1} (F'(s(mj+i)) - d_n)^2 \tag{15}$$

holds for any $j \in \mathbb{Z}^+$. For the case of chaotic dynamics, where $s(k)$ does not evolve periodically in time, this condition cannot be satisfied and equation (15) is a strict inequality.

For continuous-time systems [7, 30, 69, 70, 63, 64, 65, 67, 68], it was shown that under fast switching conditions the synchronizability of stochastically switching system can be assessed from the synchronizability of the averaged system. Here, we re-examine this limit in the case of coupled maps, whereby the averaged system is obtained by replacing the switching gain by its expected values. The synchronizability of the averaged system is ascertained by studying the Lyapunov exponent obtained by replacing $d^\star$ with $\mathrm{E}[d]$ in equation (9), that is,

$$\lambda^{\mathrm{aver}} = \lim_{k\to\infty} \frac{1}{k} \sum_{j=0}^{k-1} \ln\left[(F'(s(j)) - \mathrm{E}[d])^2\right]. \tag{16}$$

In what follows, we demonstrate through examples that the weighted average Lyapunov exponent $\bar{\lambda}$ can be positive or negative, *independent* of the value of λ^{aver}. Therefore, the averaged system does not offer valuable insight on the stability of the synchronization manifold of the stochastically coupled maps. For the sake of illustration, we consider the case in which the individual dynamics corresponds to the identity, such that

$$\begin{bmatrix} x_1(k+1) \\ x_2(k+1) \end{bmatrix} = \begin{bmatrix} x_1(k) + \varepsilon_1(k)(x_2(k) - x_1(k)) \\ x_2(k) + \varepsilon_2(k)(x_1(k) - x_2(k)) \end{bmatrix}. \tag{17}$$

In this case, the transverse dynamics in (4) takes the simple form

$$\xi(k+1) = [1 - d(k)]\,\xi(k). \tag{18}$$

Statically coupled identity maps should have a Lyapunov exponent given by (9) with $F'(s(j)) = 1$, that is,

$$\lambda^{\text{st}}(d^\star) = \ln\left[(1-d^\star)^2\right]. \tag{19}$$

Suppose that the net switching gain is a random variable that takes values $d_1 = 1$ and $d_2 = -1$ with equal probabilities 0.5. Then, using equation (19) we compute

$$\bar{\lambda} = \frac{1}{2}\left(\lambda^{\text{st}}(1) + \lambda^{\text{st}}(-1)\right) = -\infty, \tag{20a}$$

$$\lambda^{\text{aver}} = \lambda^{\text{st}}(0) = 0 > \bar{\lambda}. \tag{20b}$$

Thus, the average coupling does not support synchronization, even though the effective Lyapunov exponent is negative.

Now, we assume $d_1 = 0$ and $d_2 = 2$ with the same probability 0.5, which yields

$$\bar{\lambda} = \frac{1}{2}\left(\lambda^{\text{st}}(0) + \lambda^{\text{st}}(2)\right) = 0, \tag{21a}$$

$$\lambda^{\text{aver}} = \lambda^{\text{st}}(1) = -\infty < \bar{\lambda}. \tag{21b}$$

This posits that the stochastically coupled maps cannot synchronize for any selection of the period m, even though the average coupling affords synchronization in a single time step.

If the difference between the possible values of the net coupling gain in D is sufficiently small, the stability of the stochastic system can be related to the stability of the error dynamics of the averaged system. In this case, if for all $l = 1, \ldots, n$, we can write $F'(x) - d_l$ as $F'(x) - \Delta d_l + \mathrm{E}[d]$, where $|\Delta d_l| \ll |F'(x) - \mathrm{E}[d]|$ is the deviation of the stochastic switching with respect to their expected value. Thus, we obtain

$$\bar{\lambda} = \sum_{l=1}^{n} p_l \lim_{k\to\infty} \frac{1}{k} \sum_{j=0}^{k-1} \ln\left[(F'(s(j)) - \mathrm{E}[d] + \Delta d_l)^2\right] \approx$$
$$\lim_{k\to\infty} \frac{1}{k} \sum_{j=0}^{k-1} \left(\ln\left[(F'(s(j)) - \mathrm{E}[d])^2\right]\right) + \sum_{l=1}^{n} \lim_{k\to\infty} \sum_{j=0}^{k-1} \frac{2p_l \Delta d_l}{F'(s(j) - E[d]} = \lambda^{\mathrm{aver}}, \quad (22)$$

where we have expanded the logarithm in series in the neighborhood of $F'(s(j)) - \mathrm{E}[d]$ and we have used the fact that $\sum_{l=1}^{n} p_l \Delta d_l = 0$ by construction.

3.5 Chaotic Dynamics

Direct computation of the Lyapunov exponent as a limit of a time series from equation (8) or (11) may be challenging or even not feasible; for example, if $F'(x)$ is undefined on a finite set of points x. Following the approach of [33], we replace the summation with integration using Birkhoff's ergodic theorem [14].

Toward this aim, we introduce $\rho(x)$ as the probability density function of the map $F(x)$, defined on a set B and continuously differentiable on B except for a finite number of points. The probability density function of each map can be found analytically or numerically [9, 12]. Using Birkhoff's ergodic theorem, equations (8), (9), and (11) can be written as

$$\lambda_l^{\mathrm{st}} = \int_B \ln\left[(F'(t) - d_l)^2\right] \rho(t) dt, \quad (23a)$$

$$\lambda(m) = \int_B \ln \sum_{l=1}^{n} p_l Y_l(t,m) \rho(t) dt, \quad (23b)$$

$$\lambda(m) = m \sum_{l=1}^{n} p_l \lambda_l^{\mathrm{st}} + \int_B \ln \frac{\sum_{l=1}^{n} p_l Y_l(t,m)}{\prod_{l=1}^{n} Y_l^{p_l}(t,m)} \rho(t) dt. \quad (23c)$$

Here, we have introduced the function of time and switching period

$$Y_l(t,m) = \prod_{i=0}^{m-1} (F'(F^i(t)) - d_l)^2, \quad (24)$$

where $F^i(t) = [F \circ F \circ \ldots \circ F](t)$ is the composite function of order i.

If the analytical expression of the probability density function is known, the Lyapunov exponents can be found explicitly as further detailed in what follows when we study coupled tent maps. Numerical analysis can also benefit from the above formulation, which obviates with computational challenges related to uncertainties in rounding variables in equations (8), (9), and (11) for large values of k. This may be especially evident for large curvatures of the individual map, which could result in sudden changes in the synchronization dynamics.

Remark 3. Equation set (23) can be used to explore the synchronizability of an N-periodic trajectory $s(Nk+i)=s_i$, where $i=0,1,\ldots,N-1, k\in\mathbb{Z}^+$, and $N\in\mathbb{Z}^+/\{0\}$, by using the appropriate probability density function [12] $\rho(s)=\frac{1}{N}\sum_{i=0}^{N-1}\delta(s-s_i)$, where $\delta(\cdot)$ denotes the Dirac delta distribution. Specifically, from (23a) and (23b), we establish

$$\lambda(m)=\frac{1}{N}\sum_{i=0}^{N-1}\ln\sum_{l=1}^{n}p_lY_l(s_i,m). \tag{25}$$

3.6 A Representative Example: Coupled Tent Maps

To illustrate our approach, we use the paradigm of two linearly coupled one-dimensional tent maps. Statically coupled tent maps are known to have two symmetric ranges of positive and negative coupling for which synchronization is locally stable [33] (see Fig. 5). In our setting, we let the coupling stochastically switch between values within and outside these stability regions to explore the emergence of windows of opportunity. We will demonstrate that while fast switching, occurring at each time step may not synchronize the maps, there can be a range of lower frequencies that yields stable synchronization. We argue that this is possible for coupled maps where the probability of switching between stable and unstable configurations is uneven, inducing a non-trivial balance between the dynamics of the coupled maps and the switching periods.

The chaotic tent map, described by the equation

$$x(k+1)=F(x(k))=\begin{cases}ax(k), & x(k)<1/2\\ a(1-x(k)), & x(k)\geq 1/2\end{cases} \tag{26}$$

with parameter $a=2$ is known to have a constant invariant density function $\rho(t)=1$ [33].

3.6.1 Statically Coupled Maps

The stability of synchronization in a static network (3) of tent maps (26) is controlled by the sign of the transversal Lyapunov exponent [33]

$$\lambda^{st}=\ln|2-\varepsilon|+\ln|2+\varepsilon|. \tag{27}$$

Figure 5 indicates two disjoint regions given by $\varepsilon\in\left[-\sqrt{5},-\sqrt{2}\right]$ and $\varepsilon\in\left[\sqrt{2},\sqrt{5}\right]$ in which $\lambda^{st}<0$ and synchronization is stable.

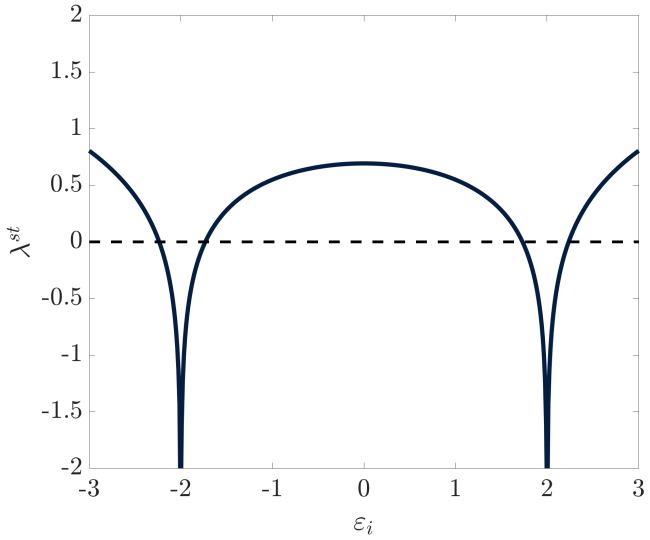

Fig. 5: Transversal Lyapunov exponent, λ^{st}, for stability of synchronization in the static network of tent maps (3), calculated through (27) as a function of coupling ε.

3.6.2 Stochastically Coupled Maps

To elucidate synchronizability of stochastically coupled tent maps, we assume that the net coupling gain d takes values d_1 and d_2 with corresponding probabilities p_1 and $p_2 = 1 - p_1$. The numerical computation of the Lyapunov exponent in (8) is performed for different values of d_2 from -4 to 4 with a step of 0.01 and m from 1 to 25 with a step of 1. The probability p_1 is held fixed to 0.5 and the net coupling gain d_1 to -1.90.

This wide parameter selection allows for exploring the connection between the stability of synchronization for static coupling and the resulting stochastic synchronization. We consider different cases, where stochastic switching is implemented on coupling gains which could individually support or hamper synchronization for statically coupled maps. Specifically, we contemplate the case in which: none (case I), one (case II), or both (case III) of the coupling gains yield synchronization.

A closed-form expression for the Lyapunov exponent of coupled tent maps can be derived from equation (23b) using the probability density function $\rho(t) = 1$, see [26] for a precise derivation,

$$\lambda(m) = \frac{1}{2^m} \sum_{i=0}^{m} \binom{m}{i} \ln \left(\sum_{l=1}^{n} p_l (2 - d_l)^{2(m-i)} (2 + d_l)^{2i} \right). \tag{28}$$

We comment that for large m the binomial coefficient grows as $2^m/\sqrt{m}$ according to Stirling's formula, which ensures that the summation is well behaved in the slow switching limit [55].

Figure 6(top) provides the Lyapunov exponent of two stochastically tent maps, analytically computed from equation (28). The effective Lyapunov exponent is directly computed from equation (27), which for the select parameters, $p_1 = p_2 = 0.5$ and $d_1 = -1.90$, yield the following intervals for

$$d_2 : \left(-\sqrt{4+\frac{1}{0.39}}, -\sqrt{4-\frac{1}{0.39}}\right) \cup \left(\sqrt{4-\frac{1}{0.39}}, \sqrt{4+\frac{1}{0.39}}\right).$$

Importantly, analytical results for large periods in Fig. 6(bottom) confirm that slow switching in case III favors stochastic synchronization. Figure 6(bottom) also confirms the existence of a thin green zone surrounding the blue bands, where synchronization is stable even though one of the coupling gains does not support synchronization (case II). For example, in the case of fast switching, $m = 1$, these regions are $(-2.33, -2.24)$ and $(-1.73, -1.64)$ from the closed-form expressions in equations (27) and (28).

The analytical solution in equation (28) allows for shedding further light on the possibility of synchronizing coupled maps in case II. Specifically, in Fig. 7 we consider switching between coupling gains $d_1 = -1.9999$ and $d_2 = 1.7000$, which are associated with $\lambda_1^{\text{st}} = -7.82$ (strongly stable synchronization) and $\lambda_2^{\text{st}} = 0.10$ (weakly unstable synchronization). We systematically vary the probability of switching p_1 from 0.6 to 1 with a step 0.001, so that when the coupled maps spend most of the time with the coupling gain that would support synchronization. In this case, the effective Lyapunov exponent is always negative, and synchronization may be attained everywhere in the parameter space.

Surprisingly, under fast switching conditions, synchronization is not attained if $p_1 \lessapprox 1$ as shown in Fig. 7. Although the maps spend most of the time in a configuration that would strongly support synchronization, the sporadic ($p_2 \approx 0$) occurrence of a coupling gain which would lead to weak instability hampers stochastic synchronization under fast switching. Increasing the switching period, synchronization may be attained for $p_1 > 0.995$ (see the "Pinocchio nose" in Fig. 7(bottom)). For $0.753 < p_1 < 0.795$, we observe a single window of opportunity, whereby synchronization is achieved in a compact region around $m = 10$. For $0.795 \lessapprox p_1 \lessapprox 0.824$, a second window of opportunity emerges for smaller values of m around 5. The two windows ultimately merge for $p_1 \approx 0.83$ in a larger window that grows in size as p_1 approaches 1.

In summary, we have studied the stochastic stability of the transverse dynamics using the notion of mean square stability, establishing a mathematically-tractable form for the Lyapunov exponent of the error dynamics. We have demonstrated the computation of the stochastic Lyapunov exponent from the knowledge of the probability density function. A necessary condition for stochastic synchronization has been established, aggregating the Lyapunov exponents associated with each static coupling configuration into an effective Lyapunov exponent for the stochastic dy-

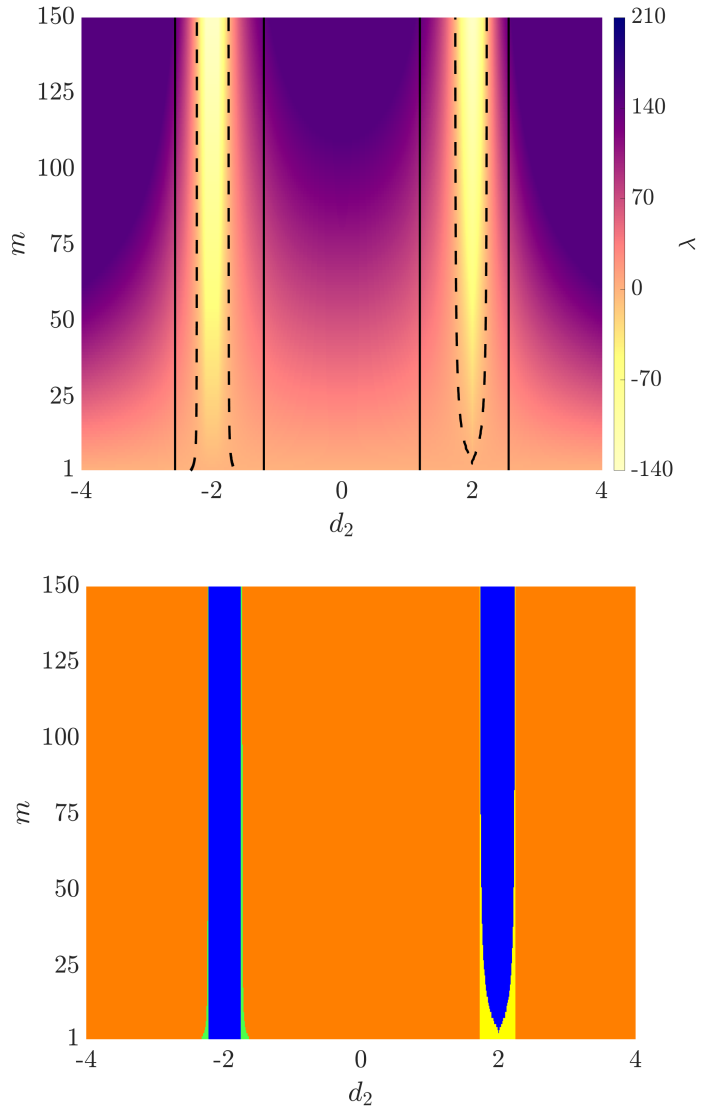

Fig. 6: Analytical demonstration of synchronization through non-fast switching. (top) Lyapunov exponent of two stochastically tent maps, where the net coupling is switching with equal probability between $d_1 = -1.90$ and d_2 at a period m, analytically computed from equation (28). The color bar illustrates the range of Lyapunov exponents attained for each value of γ. The dashed line identifies the values of d_2 and m for which the Lyapunov exponent is zero; the regions within such contours correspond to negative values of the Lyapunov exponent and thus stochastic synchronization. The solid lines refer to the values of d_2 and m for which the effective Lyapunov exponent is zero. The vertical bands identified by such solid lines correspond to regions where stochastic synchronization is feasible, as predicted by Proposition 3.1. (bottom) Interplay between synchronization in stochastically and statically coupled tent maps. The partition into cases I, II, and III is based on the sign of the Lyapunov exponent in equation (27), corresponding to the net couplings d_1 and d_2. The regions are colored as follows: orange (case II without stochastic synchronization); yellow (case III without stochastic synchronization); green (case II with stochastic synchronization); and blue (case III with stochastic synchronization).

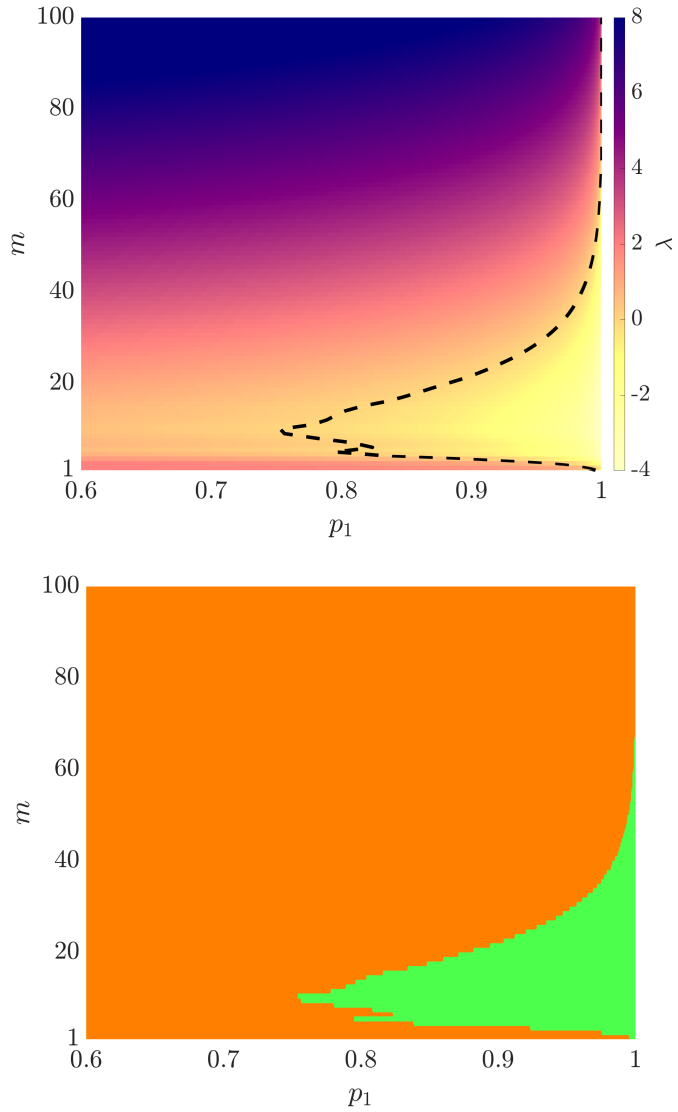

Fig. 7: Analytical demonstration of emergence of windows of opportunity. (top) Lyapunov exponent of two stochastically tent maps as a function of the switching probability p_1 and the period m, analytically computed from equation (28) with $d_1 = -1.9999$ and $d_2 = 1.7000$. The color bar illustrates the range of Lyapunov exponents attained for each value of γ. The dashed line identify the values of d_2 and m for which the Lyapunov exponent is zero; the regions within such contours correspond to negative values of the Lyapunov exponent and thus stochastic synchronization. (bottom) Interplay between synchronization in stochastically and statically coupled tent maps. For the select values of the net couplings, $\lambda_1^{st} = -7.82$ and $\lambda_2^{st} = 0.10$, which correspond to case II. The regions are colored as follows: orange (case II without stochastic synchronization) and green (case II with stochastic synchronization).

namics. For tent maps, we have established a closed-form expression for the stochastic Lyapunov exponent, which helps dissecting the contribution of the coupling gains, switching probabilities, and switching period on stochastic synchronization.

We have demonstrated that non-fast switching may promote synchronization of maps whose coupling alternates between one configuration where synchronization is unstable and another where synchronization is stable (case II). These windows of opportunity for the selection of the switching period may be disconnected and located away from the fast switching limit, where the coupling is allowed to change at each time step.

In contrast to one's expectations, fast switching may not even be successful in synchronizing maps that are coupled by switching between two configurations that would support synchronization (case III). However, a sufficiently slow switching that allows the maps to spend more time in one of the two stable synchronization states will induce stochastic synchronization. The emergence of a lower limit for the switching period to ensure stochastic synchronization is highly non-trivial, while the stabilization of synchronization by slow switching in the dwell time limit should be expected as the maps will spend the time necessary to synchronize in one of the stable configurations, before being re-wired to the other stable configuration.

4 Network Synchronization Through Stochastic Broadcasting

Building on our results from the previous section on the stochastic synchronization of two intermittently coupled maps, in this section, we go further and address an important problem of how non-fast switching can be used to control synchronization in a target network through stochastic broadcasting from a single external node.

This problem of controlling synchronous behavior of a network towards a desired common trajectory [52] arises in many technological and biological systems where agents are required to coordinate their motion to follow a leader and maintain a desired formation [71]. In our setting, each node of the target network, implemented as a discrete-time map, is coupled to the external node with connections that stochastically switch in time with an arbitrary switching period. The network is harder to synchronize than its isolated nodes, as its structure contributes to resilience to controlled synchronization probed by the externally broadcasting node.

In the following, we will rigorously study the mean square stability of the synchronous solution in terms of the error dynamics and provide an explicit dependence of the stability of controlled synchronization on the network structure and the properties of the underlying broadcasting signal, defined by the strength of broadcasting connections and their switching period and probability. Via an analytical treatment of the Lyapunov exponents of the error dynamics and the use of tools from ergodic theory, we derive a set of stability conditions that provide an explicit criterion on how the switching period should be manipulated to overcome network resilience to synchronization as a function of the Laplacian spectrum of the network [25].

Through the lens of chaotic tent maps, we discover that the network topology shapes the windows of opportunity of favorable non-fast switching in a highly nonlinear fashion. In contrast to mutual synchronization with a network whose stability is determined by the second smallest and largest eigenvalue of the Laplacian matrix via the master stability function, [57] controlled synchronization by the external node is defined by *all its eigenvalues*, including the zero eigenvalue. In the case of chaotic tent maps, the zero and the largest eigenvalue appear to effectively control the size of these windows of opportunity. This leads to the appearance of a persistent window of favorable switching periods where all network topologies sharing the largest eigenvalue become more prone to controlled synchronization.

We study the synchronization of a network of N discrete-time oscillators given by the state variables $y_i \in \mathbb{R}$ for $i = 1, 2, \ldots, N$ [1] that are driven by an external reference node given by $x \in \mathbb{R}$ via a signal that is stochastically broadcasted to all of the nodes in the network. The topology of the network is undirected and unweighted. It is described by the graph $\mathscr{G} = (\mathscr{V}, \mathscr{E})$, where $\mathscr{V}$ is the set of vertices and $\mathscr{E}$ is the set of edges. The broadcaster-network system is depicted in Fig. 8. The evolution of the oscillators in the network and the reference node are given by the same mapping function $F : \mathbb{R} \to \mathbb{R}$, such that $x(k+1) = F(x(k))$. The switching of the broadcasted signal is an independent and identically distributed (i.i.d) stochastic process that reswitches every m time steps. That is, the coupling strength of the reference node $\varepsilon(mk) = \varepsilon(mk+1) = \cdots = \varepsilon(m(k+1)-1)$ is drawn randomly from a set of n coupling strengths $\{\varepsilon_1, \ldots, \varepsilon_n\}$ with probabilities $p_1, \ldots, p_n$, respectively ($\sum_{l=1}^{n} p_l = 1$).

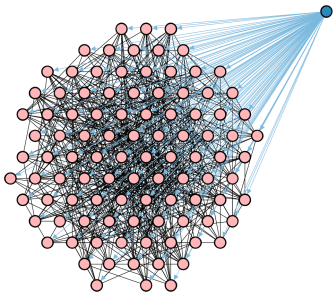

Fig. 8: The reference node (blue) stochastically broadcasts a signal to each of the nodes in a static network of N oscillators (pink).

The evolution of the discrete-time broadcaster-network system can be written compactly as

[1] These results generalize for $y_i \in \mathbb{R}^n$.

$$\begin{aligned} x(k+1) &= F(x(k)), \\ \mathbf{y}(k+1) &= \mathbf{F}(\mathbf{y}(k)) - \mu L\mathbf{y}(k) - \varepsilon(k) I_N (\mathbf{y}(k) - x(k)\mathbf{1}_N), \end{aligned} \tag{29}$$

where $\mathbf{F}$ is the natural vector-valued extension of F, μ is the coupling strength within the network, $\mathbf{1}_N$ is the vector of ones of length N, I_N is the $N \times N$ identity matrix, and L is the Laplacian matrix of $\mathscr{G}$ i.e., $L_{ij} = -1$ for $ij \in \mathscr{E}$, $L_{ii} = -\sum_{j=1, j\neq i}^{N} L_{ij}$, $i = 1, 2, \ldots, N$. Without loss of generality, we order and label the Laplacian spectrum of L: $\gamma_1 = 0 \leq \gamma_2 \leq \cdots \leq \gamma_N$.

We study the stability of the stochastic synchronization of the network about the reference node's trajectory, or $y_1(k) = y_2(k) = \cdots = y_N(k) = x(k)$. Towards this goal, it is beneficial to re-format the problem and study the evolution of the error dynamics $\xi(k) = x(k)\mathbf{1}_N - \mathbf{y}(k)$. When all of the nodes $y_i(k)$ have converged to the reference trajectory, $\xi(k) = x(k)\mathbf{1}_N - \mathbf{y}(k) = \mathbf{0}_N$. To study the stability of synchronization, we linearize the system about the reference trajectory

$$\xi(k+1) = [DF(x(k))I_N - \mu L - \varepsilon(k)I_N]\,\xi(k), \tag{30}$$

where $DF(x(k))$ is the Jacobian of F evaluated along the reference trajectory $x(k)$. As is typical of linearization, we assume that the perturbations $\xi_i(k)$ in the variational equation (30) are small and in directions transversal to the reference trajectory. Convergence to the reference trajectory along these transversal directions ensures the local stability of the synchronous solution. Despite the stochastic and time-dependent nature of the broadcasting signal $\varepsilon(k)$, it only appears on the diagonal elements underlying the evolution of the error vector $\xi(k)$. Because μL is the only matrix in (30) that is not diagonal, we can diagonalize (30) with respect to the eigenspaces of the Laplacian matrix.

We obtain the stochastic master stability equation

$$\zeta(k+1) = [DF(x(k)) - \mu\gamma - \varepsilon(k))]\,\zeta(k), \tag{31}$$

where $\gamma \in \{\gamma_1, \ldots, \gamma_N\}$ and $\zeta \in \mathbb{R}$ is a generic perturbation along the eigendirection of L. Notice that $\gamma_1 = 0$ corresponds to the evolution of the error dynamics in the absence of a network. Lastly, in order to simplify the analysis of the evolution of the variational equations, we re-scale the time variable with respect to the switching period

$$\tilde{\zeta}(k+1) = \prod_{i=0}^{m-1} [DF(x(mk+i)) - \mu\gamma - \tilde{\varepsilon}(k)]\,\tilde{\zeta}(k), \tag{32}$$

where $\tilde{\zeta}(k) = \zeta(mk)$ and $\tilde{\varepsilon}(k) = \varepsilon(mk)$. This scalar equation provides the explicit dependence of the synchronization error on the network topology (via $\mu\gamma$) and the strength of the broadcasted signal (via ε). With this in mind, we continue by discussing the stability of the synchronization to the reference trajectory.

Definition 4.1. The synchronous solution $y_i(k) = x(k)$ for $i = 1, 2, \ldots, N$ in the stochastic system (29) is *locally mean square asymptotically stable* if $\lim_{k\to\infty} \mathrm{E}[\tilde{\zeta}^2(k)] =$

0 for any $\tilde{\zeta}(0)$ and $\gamma \in \{\gamma_1, ..., \gamma_N\}$ in (32), where $\mathrm{E}[\cdot]$ denotes expectation with respect to the σ-algebra generated by the stochastic process underlying the switching.

Mean square stability of the stochastic system in (32), and by extension synchronization in the original system (29), corresponds to studying the second moment of $\tilde{\zeta}(k)$. We take the expectation of the square of the error in (32)

$$\mathrm{E}[\tilde{\zeta}^2(k+1)] = \sum_{l=1}^{n} p_l \left(\prod_{i=0}^{m-1} \left[DF(x(mk+i)) - \mu\gamma - \varepsilon_l \right] \right)^2 \mathrm{E}[\tilde{\zeta}^2(k)]. \tag{33}$$

Reducing the stochastically switching system (29) to a deterministic system (33) allows for the use of standard tools from stability theory, such as Lyapunov exponents [56]. The Lyapunov exponent for (33) is computed as

$$\lambda = \lim_{k\to\infty} \tfrac{1}{k} \ln \left[\frac{\mathrm{E}[\tilde{\zeta}^2(k)]}{\tilde{\zeta}^2(0)} \right] = \lim_{j\to\infty} \tfrac{1}{j} \sum_{k=1}^{j} \ln \left[\mathrm{E}[\tilde{\zeta}^2(k+1)] \right]. \tag{34}$$

There are numerous pitfalls that can undermine the numerical computation of Lyapunov exponent from a time series, such as $\mathrm{E}[\tilde{\zeta}^2]$ falling below numerical precision in a few time steps and incorrectly predicting stochastic synchronization for trajectories that would eventually diverge. With the proper assumptions, one can use Birkoff's ergodic theorem [56] to avoid these confounds and form the main analytical result of this section.

Proposition 4.1. *The synchronous solution $x(k)$ of the stochastic system (29) is locally mean square asymptotically stable if*

$$\lambda = \int_B \ln \left[\sum_{l=1}^{n} p_l \left(\prod_{i=0}^{m-1} \left[DF(t) - \mu\gamma - \varepsilon_l \right] \right)^2 \right] \rho(t) dt \tag{35}$$

is negative for $\forall \gamma \in \{\gamma_1, \ldots, \gamma_N\}$. Here, B is the region for which the invariant density $\rho(t)$ of F is defined.

Proof. Assuming F is ergodic with invariant density $\rho(t)$, one can avoid computing the Lyapunov exponent from a time series using Birkoff's ergodic theorem to replace the averaging over time with averaging over the state. This amounts to replacing the summation with integration in (34). Then, by virtue of (34) and the definition of a Lyapunov exponent, stability of the stochastic system reduces to monitoring the sign of this Lyapunov exponent. □

Remark 4. We reduce studying the stability of synchronization in (29) to monitoring the sign of the Lyapunov exponents in (35), with a different exponent for each eigenvalue γ. If each of these Lyapunov exponents is negative, the dynamics of the network in the original system (29) converges to the dynamics of the reference trajectory. Furthermore, this allows the stability of stochastic synchronization to be studied explicitly in the network and broadcasting parameters μ, $\{\gamma_1, \ldots, \gamma_N\}$, $\{\varepsilon_1, \ldots, \varepsilon_n\}$, $\{p_1, \ldots, p_n\}$, and m.

Remark 5. There are two notable consequences of the Laplacian spectrum on the stability conditions given by the sign of (35): (i) $\mu\gamma = 0$ is always an eigenvalue, such that it is necessary that the nodes in the network pairwise synchronize to the reference node in the absence of a network topology, and (ii) if the network is disconnected, fewer stability conditions need to be satisfied, whereby there will be repeated zero eigenvalues. In light of these consequences, a network is inherently resilient to broadcasting synchronization, in that it necessitates satisfying more stability conditions, and synchronization in the absence of a network is always one of the stability conditions.

4.1 Tent Maps Revisited

To explore some of the theoretical implications of the general stability criterion (35), we consider the broadcaster-network system (29) composed of chaotic tent maps. In this context, the general criterion (35) can be written in a compact form that depends only on the network and broadcasting parameters.

Proposition 4.2. *A stochastic system (29) of chaotic tent maps is locally mean square asymptotically stable if*

$$\lambda = \frac{1}{2^m}\sum_{i=0}^{m}\binom{m}{i}\ln\left[\sum_{l=1}^{n} p_l Y(i,m,\mu\gamma,\varepsilon_l)\right] \tag{36}$$

is less than zero, where $Y(i,m,\mu\gamma,\varepsilon_l)$ *is given by* $(2+\mu\gamma+\varepsilon_l)^{2i}(2-\mu\gamma-\varepsilon_l)^{2(m-i)}$ *and* $\binom{m}{i} = \frac{m!}{(m-i)!i!}$.

Remark 6. The closed-form analytical expression (36) for the Lyapunov exponents indicates the explicit dependence of the stability of controlled synchronization on the network coupling strength μ, the eigenvalues of the Laplacian matrix for the network, the switching period m, the stochastically switching coupling strengths $\{\varepsilon_1,\ldots,\varepsilon_n\}$, and their respective probabilities $\{p_1,\ldots,p_n\}$. For controlled synchronization to be mean square stable, the Lyapunov exponent for each eigenvalue in the Laplacian spectrum must be negative.

To illustrate the power of our explicit criterion (36) for controlled synchronization and clearly demonstrate of the emergence of windows of opportunity, we limit our attention to stochastic broadcasting between two coupling strengths ε_1 (with probability p) and ε_2 (with probability $1-p$).

To choose the coupling strengths ε_1 and ε_2, we consider two statically coupled tent maps (26)

$$\begin{aligned} x(k+1) &= f(x(k)),\\ y(k+1) &= f(y(k)) + \varepsilon(x(k)-y(k)). \end{aligned} \tag{37}$$

This network (37) describes a pairwise, directed interaction between the dynamics of the broadcasting map $x(k)$ and a single, isolated map $y(k)$ from the network where

the switching broadcasting coupling is replaced with a static connection of strength ε. The stability of synchronization in the static network (37) is controlled by the sign of the transversal Lyapunov exponent[33] given in (27). Figure 5 indicates two disjoint regions given by $\varepsilon \in \left[-\sqrt{5},-\sqrt{2}\right]$ and $\varepsilon \in \left[\sqrt{2},\sqrt{5}\right]$ in which $\lambda^{st} < 0$ and synchronization is stable.

4.2 Stochastic Broadcasting: Fast Switching ($m = 1$)

When switching occurs at every time step, the condition described in Proposition 4.2 can be simplified to the following corollary, which we state without additional proof.

Corollary 4.1. *The Lyapunov exponent for the mean square stability of the synchronous solution in the fast-switching system represented by (29) of chaotic tent maps is*

$$\lambda = \ln\left[(2-\mu\gamma)^2 + 2(\mu\gamma-2)\mathrm{E}[\varepsilon(k)] + \mathrm{E}[\varepsilon^2(k)]\right] \cdot \left[(-2-\mu\gamma)^2 + 2(\mu\gamma+2)\mathrm{E}[\varepsilon(k)] + \mathrm{E}[\varepsilon^2(k)]\right], \quad (38)$$

where $\mathrm{E}[\varepsilon(k)] = p_1\varepsilon_1 + p_2\varepsilon_2$ *and* $\mathrm{E}[\varepsilon^2(k)] = p_1\varepsilon_1^2 + p_2\varepsilon_2^2$.

4.2.1 Master Stability Function

The Lyapunov exponent (38) demonstrates the explicit dependence of the stability of stochastic synchronization on the node-to-node coupling strength, the eigenvalues of the Laplacian matrix, and the stochastically switching coupling strengths along with their respective probabilities.

Figure 9 illustrates the dependence of λ on ε_1 and $\mu\gamma$. The dashed curve in Fig. 9 indicates the boundary between positive and negative Lyapunov exponents, identifying the onset of mean square stability of the error dynamics. In order for the network to synchronize to the reference node, the point $(\varepsilon_1, \mu\gamma)$ must fall within the dashed curve for *every* eigenvalue in the spectrum of the Laplacian matrix. In agreement with our predictions, we find that as $\mu\gamma$ increases the range of values of ε_1 which affords stable synchronization becomes smaller and smaller. This suggests that the resilience of the network to synchronize improves with $\mu\gamma$.

Remark 7. While the nonlinear dependence of the stability boundary on ε_1 and $\mu\gamma$ is modulated by the nonlinearity in the individual dynamics, it should not be deemed as a prerogative of nonlinear systems. As shown in Remark 4, the stochastic stability of synchronization in the simplest case of a linear system is also nonlinearly related to the spectrum of the Laplacian matrix and to the expectation and variance of the broadcasting signal – even for classical consensus with $\alpha = 1$ [16].

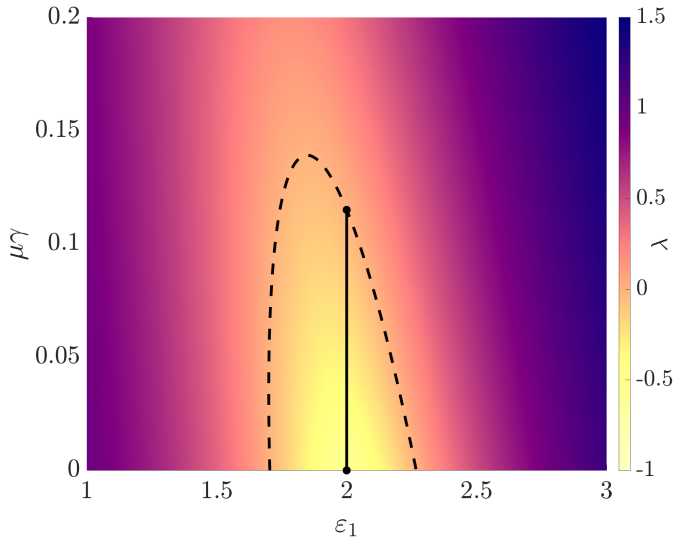

Fig. 9: Master stability function for stochastic synchronization of chaotic tent maps, for $\varepsilon_2 = 2.2, m = 1$, and $p_1 = p_2 = 0.5$. For synchronization to be stable, each eigenvalue of the Laplacian matrix must correspond to a negative Lyapunov exponent (indicated by the yellow color, isolated by the black dashed curve). For example, the black vertical line shows the range of admissible values of $\mu\gamma$ that would guarantee stability at $\varepsilon_1 = 2$.

Remark 8. In this example of a chaotic tent map, the stability boundary is a single curve, defining a connected stability region. To ensure stable synchronization of a generic network, it is thus sufficient to monitor the largest eigenvalue of the Laplacian matrix, γ_N, such that $(\varepsilon_1, \mu\gamma)$ will fall within the stability region. This is in contrast with the master stability function for uncontrolled, spontaneous synchronization [57], which would typically require the consideration of the second smallest eigenvalue, often referred to as the algebraic connectivity [25]. However, similar to master stability functions for uncontrolled, spontaneous synchronization [75], we would expect that for different maps, one may find several disjoint regions in the $(\varepsilon_1, \mu\gamma)$-plane where stable stochastic synchronization can be attained.

4.2.2 Role of Network Topology

The master stability function in Fig. 9 shows that both μ and γ contribute to the resilience of the network to synchronization induced by stochastic broadcasting. For a given value of the node-to-node coupling strength μ, different networks will exhibit different residences based on their topology. Based on the lower bound by

Grone and Merris [29] and the upper bound by Anderson and Morley [2], for a graph with at least one edge, we can write $\max\{d_i, \quad i = 1,\dots,N\} + 1 \leq \gamma_N \leq \max\{d_i + d_j, \quad ij \in \mathscr{E}\}$, where d_i is the degree of node $i = 1,\dots,N$. While these bounds are not tight, they suggest that the degree distribution has a key role on γ_N. For a given number of edges, one may expect that networks with highly heterogeneous degree distribution, such as scale-free networks [11], could lead to stronger resilience to broadcasting as compared to regular or random networks, with more homogenous degree distributions [11].

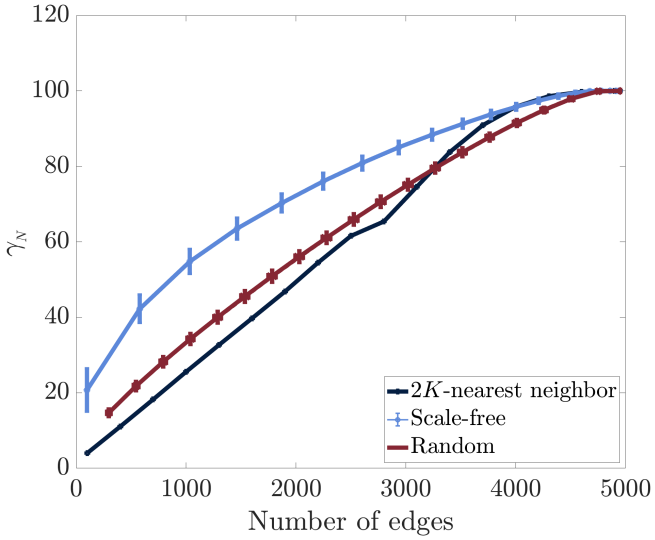

Fig. 10: Largest eigenvalue γ_N of the Laplacian matrix as a function of the number of edges for three different types of networks of 100 nodes: a $2K$-regular network (navy curve), scale-free (light blue curve), and random Erdős-Rényi (red curve) networks. Scale-free and random networks are run 10000 times to compute means and standard deviations, reported herein – note that error bars are only vertical for scale-free networks since the number of edges is fully determined by q, while for random networks also horizontal error bars can be seen due to the process of network assembly.

In Fig. 10, we illustrate this proposition by numerically computing the largest eigenvalue of the graph Laplacian for three different network types:

(i) A $2K$-regular network, in which each node is connected to $2K$ nearest neighbors, such that the degree is equal to $2K$. As K increases, the network approaches a complete graph.

(ii) A scale-free network [4] which is grown from a small network of q nodes. At each iteration of the graph generation algorithm, a node is added with q edges

to nodes already in the network. The probability that an edge will be connected to a specific node is given by the ratio of its degree to the total number of edges in the network. Nodes are added until there are N nodes in the network. When q is small, there are a few hub nodes that have a large degree and many secondary nodes with small degree, whereas when q is large, the scale-free network is highly connected and similar to a complete graph.

(iii) A random Erdős-Rényi network which takes as input the probability, p, of an edge between any two nodes. When p is small, the network is almost surely disconnected, and when p approaches 1, it is a complete graph.

We fix N to 100 and vary K, q, and p in (i), (ii), and (iii), respectively, to explore the role of the number of edges.

As expected from the bounds in [29, 2], for a given number of edges, the scale-free network tends to exhibit larger values of γ_N. This is particularly noticeable for networks of intermediate size, whereby growing the number of edges will cause the three network types to collapse on a complete graph of N nodes. As the largest eigenvalue of the Laplacian matrix fully controls the resilience of the network to broadcasting-induced synchronization (in the case of linear and chaotic tent maps), we may argue that, given a fixed number of edges, the network can be configured such that it is either more conducive (regular graph) or resistant (scale-free graph) to synchronization. The increased resilience of scale-free networks should be attributed to the process of broadcasting-induced synchronization, which globally acts on all nodes simultaneously, without targeting critical nodes (low or high degree) like in pinning control [16, 78].

4.3 Stochastic Broadcasting: Beyond Fast Switching ($m > 1$)

Returning to the stochastically switching broadcaster-network system, but without the limitation of $m = 1$, we use the master stability function of Fig. 5 to choose $\varepsilon_1 = -1.999$ from a stability region and $\varepsilon_2 = -1.7$ from an instability region such that the connection from the broadcasting node to the network switches between the two values where one value supports controlled synchronization whereas the other destabilizes it. In this way, the broadcaster sends two conflicting messages to the network to follow and not to follow its trajectory.

We pay particular attention to the case where the switching probability of the stabilizing coupling, ε_1 is higher ($p > 0.5$.) One's intuition would suggest that fast-switching between the stable and unstable states of controlled synchronization with probability ($p > 0.5$), that makes the system spend more time in the stable state, would favor the stability of synchronization. However, the master stability function of Fig. 11 calculated through the analytical expression for the Lyapunov exponent (36) shows that this is not the case. Our results reveal the presence of a stability zone (black area) which, in terms of the switching periods m, yields a window of opportunity when non-fast switching favors controlled synchronization, whereas fast or slow switching does not. The fact that slower switching at $m > 25$ at the switching

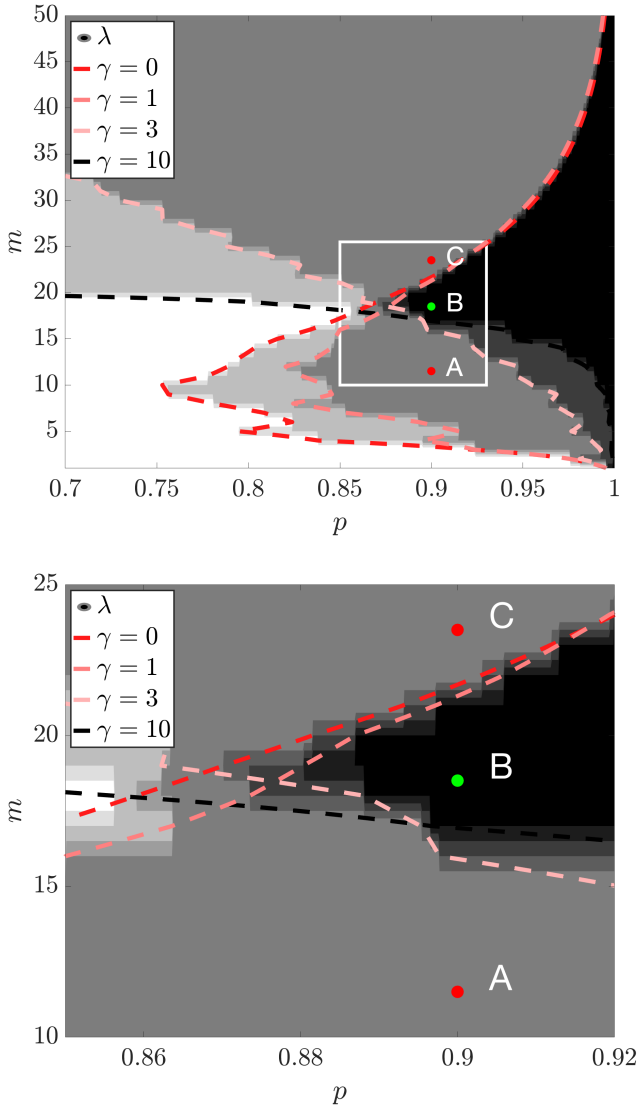

Fig. 11: Analytical calculation of the master stability function (36) for controlled synchronization of tent maps as a function of the switching probability p and switching period m for $\varepsilon_1 = -1.9999, \varepsilon_2 = 1.7$, and $\mu = 0.01$. (Top). The black region indicates the stability of controlled synchronization, and the dashed lines represent the boundaries for the stability region for various eigenvalues γ of a network's Laplacian matrix. Notice that the size of the stability region is primarily controlled by only two curves, corresponding to $\gamma = 0$ (red dashed) and $\gamma = 10$ (black dashed) such that the addition of curves for eigenvalues $\gamma \in (0, 10)$ only affects the small cusp part of the stability region (see the zoomed-in area). (Bottom). Zoom-in of the region marked by the white rectangle in (top). Points A, B, and C indicate pairs (p, m) for which synchronization is unstable, stable, and unstable, respectively for different values of the switching period m. Note the window of favorable frequencies m which includes point B in the vertical direction from A to C. Remarkably, the size of the stability region remains persistent to changes of the intra-network coupling μ (not shown), suggesting the existence of soft, lower and upper thresholds for favorable switching frequencies between $m = 20$ and 30.

probability $p = 0.9$ (see the transition from point A to B) desynchronizes the system is somewhat unexpected, as the system is likely to stay most of the time in the stable state, defined by ε_1.

The exact cause of this effect remains to be studied; however, we hypothesize that this instability originates from a large disparity between the time scale of weak convergence in the vicinity of the synchronization state during the (long) time lapse when the stabilizing coupling ε_1 is on and the time scale of strong divergence from the synchronization solution far away from it when the destabilizing coupling ε_2 finally switches on. As a result, this unbalance between the convergence and divergence makes synchronization unstable.

The window of opportunity displayed in Fig. 11 appears as a result of intersections between the boundaries (dashed curves) of the stability zones where each boundary is calculated from the criterion (36) when the Lyapunov exponent is zero for each eigenvalue of the Laplacian matrix. The red curve for $\gamma_1 = 0$ shows the stability region in the absence of a network, and is therefore a necessary condition for controlled synchronization in the presence of the network. In the general case of N distinct eigenvalues, there will be N curves. Each curve adds a constraint and, therefore, one would expect each eigenvalue $\gamma_1, \ldots, \gamma_N$ to play a role in reducing the size of the stability zone and shaping the window of opportunity as a function of network topology.

In contrast to these expectations, Fig. 11 provides a convincing argument that the stability zone is essentially defined by two curves, corresponding to the zero eigenvalue, γ_1 (red dashed curve) and the largest eigenvalue, γ_N (black dashed curve). All the other curves offer a very minor contribution to shaping the stability region. As a consequence, windows of opportunity should be relatively robust to topological changes, preserving the maximum largest eigenvalue of the Laplacian spectrum. For example, the set of four distinct eigenvalues $(0,1,3,10)$ in Fig. 11 corresponds to a star network of 10 nodes with an additional edge connecting two outer nodes. In this case, the removal of the additional link reduces the spectrum to three distinct eigenvalues $(0,1,10)$ and eliminates the curve for $\gamma = 3$ which, however, does not essentially change the stability region. This observation suggests that the addition of an edge to a controlled network, which would be expected to help a network better shield from the external influence of the broadcasting node, might not necessarily improve network resilience to synchronization.

Similarly, the removal of an edge from an all-to-all network with two distinct eigenvalues $(0,N)$ changes the spectrum to $(0,N-1,N)$, which according to Fig. 11 does not significantly alter the stability region either. For general topologies, one may look at the degree distribution to gather insight on the largest eigenvalue[2, 29], thereby drawing conclusions on the switching periods that guarantee the success of the broadcaster to synchronize the network. Put simply, "you can run but you cannot hide:" the broadcaster will identify suitable switching rates to overcome the resilience of the network.

5 Conclusions

While the study of stochastically switching networks has gained significant momentum, most analytical results have been obtained under the assumption that the characteristic time scales of the intrinsic oscillators and evolving connections are drastically different, enabling the use of averaging and perturbation methods. In regard to on-off stochastically switching systems, these assumptions typically yield two extremes, fast or slow (dwell-time [35]) switching, for which rigorous theory has been developed [31, 32, 5, 7, 70, 69, 67, 63]. However, our understanding of dynamical networks with non-fast switching connections is elusive, and the problem of an analytical treatment of the dynamics and synchronization in non-fast switching network remains practically untouched.

In this chapter, we sought to close this gap by presenting an analytical approach to characterize the stability of synchronization in stochastically switching networks of discrete-time oscillators as a function of network topology and switching period. We first focused on the simplest stochastic network composed of two maps and studied the stability of synchronization by analyzing the linear stability of an augmented system, associated with the linear mean square transverse dynamics. We performed a detailed analysis of the Lyapunov exponent of the transverse dynamics, based on the knowledge of the probability density function for the synchronized trajectory. We established a necessary condition for stochastic synchronization in terms of the synchronizability of the coupled maps with a static coupling. The necessary condition can be used to demonstrate that switching between configurations which do not individually support synchronization will not stabilize stochastic synchronization for any switching frequencies. This is in contrast with networks of continuous-time oscillators where windows of opportunity for stable synchronization may appear as a result of switching between *unstable states* [40, 41]. Through closed-form and numerical findings, we have demonstrated the emergence of windows of opportunity and elucidated their nontrivial relationship with the stability of synchronization under static coupling.

While the details of the mechanisms for the appearance of windows of opportunity in stochastically switching networks are yet to be clarified, it is tenable to hypothesize that this effect is related to the dynamic stabilization of an unstable state. From a mechanics perspective, this can be loosely explained by an analogy to the dynamics of Kapitza's pendulum. Kapitza's pendulum is a rigid pendulum in which the pivot point vibrates in a vertical direction, up and down [43]. Stochastic vibrations of the suspension are known to stabilize Kapitza's pendulum in an upright vertical position, which corresponds to an otherwise unstable equilibrium in the absence of suspension vibrations. By this analogy, stochastic switching between stable and unstable configurations can be proposed to perform a similar stabilizing role.

Extending our analysis of synchronization of two maps, we then established a rigorous toolbox for assessing the mean-square stability of controlled synchronization in a static network of coupled maps induced by stochastic broadcasting from a single, external node. We studied the conditions under which a reference broadcasting

node can synchronize a target network by stochastically transmitting sporadic, possibly conflicting signals. We demonstrated that manipulating the rate at which the connections between the broadcasting node and the network stochastically switch can overcome network resilience to synchronization. Through a rigorous mathematical treatment, we discovered a nontrivial interplay between the network properties that control this resilience and the switching rate of stochastic broadcasting that should be adapted to induce synchronization. Unexpectedly, non-fast switching rates controlling the so-called windows of opportunity guarantee stable synchrony, whereas fast or slow switching leads to desynchronization, even though the networked system spends more time in a state favorable to synchronization.

In contrast to classical master stability functions for uncontrolled synchronization, where both the algebraic connectivity and the largest eigenvalue of the Laplacian matrix determine the onset of synchronization, we report that the algebraic connectivity has no role on broadcasting-induced synchronization of chaotic tent maps. Specifically, the resilience of the network to broadcasting synchronization increases with the value of the largest eigenvalue of the Laplacian matrix. Heterogenous topologies with hubs of large degree should be preferred over homogenous topologies, when designing networks that should be resilient to influence from a broadcasting oscillator. On the contrary, homogenous topologies, such as regular or random topologies, should be preferred when seeking networks that could be easily tamed through an external broadcasting oscillator. Interestingly, these predictions would be hampered by a simplified analysis based on averaging, which could lead to false claims regarding the stability of synchronous solutions.

Our approach is directly applicable to high-dimensional maps whose invariant density measure can calculated explicitly. These systems include two-dimensional diffeomorphisms on tori such as Anosov maps [34], for which the invariant density measure can be calculated analytically, and volume-preserving two-dimensional standard maps whose invariant density function can be assessed through computer-assisted calculations [45]. Although our work provides an unprecedented understanding of network synchronization beyond the fast switching limit, we have hardly scratched the surface of temporal dynamical networks theory. This work immediately raises the following questions: (i). What if the i.i.d process underlying the switching was relaxed to be a more general Markov process? (ii). What if the underlying topology of the broadcasting was more complex? Both of these questions are of interest, but provide their own technical challenges and require further study. We anticipate that combining our recent work on synchronization of two maps under Markovian switching with memory [62] with the approach presented in this chapter should make progress toward unraveling a complex interplay between switching memory and network topology for controlled synchronization.

6 Acknowledgements

This work was supported by the U.S. Army Research Office under Grant No. W911NF-15-1-0267 (to I.B., R.J., and M.P.), the National Science Foundation (USA) under Grants No. DMS-1009744 and DMS-1616345 (to I.B and R.J.), and CMMI 1561134, CMMI 1505832, and CMMI 1433670 (to M.P.).

References

1. Nicole Abaid and Maurizio Porfiri. Consensus over numerosity-constrained random networks. *IEEE Transactions on Automatic Control*, 56(3):649–654, 2011.
2. William N Anderson Jr and Thomas D Morley. Eigenvalues of the laplacian of a graph. *Linear and Multilinear Algebra*, 18(2):141–145, 1985.
3. Alex Arenas, Albert Díaz-Guilera, Jurgen Kurths, Yamir Moreno, and Changsong Zhou. Synchronization in complex networks. *Physics Reports*, 469(3):93–153, 2008.
4. Albert-László Barabási and Réka Albert. Emergence of scaling in random networks. *Science*, 286(5439):509–512, 1999.
5. Igor Belykh, Vladimir Belykh, Russell Jeter, and Martin Hasler. Multistable randomly switching oscillators: The odds of meeting a ghost. *The European Physical Journal Special Topics*, 222(10):2497–2507, 2013.
6. Igor Belykh, Mario Di Bernardo, Jürgen Kurths, and Maurizio Porfiri. Evolving dynamical networks. *Physica D: Nonlinear Phenomena*, 267(1):1–6, 2014.
7. Igor V Belykh, Vladimir N Belykh, and Martin Hasler. Blinking model and synchronization in small-world networks with a time-varying coupling. *Physica D: Nonlinear Phenomena*, 195(1):188–206, 2004.
8. Vladimir N Belykh, Igor V Belykh, and Martin Hasler. Connection graph stability method for synchronized coupled chaotic systems. *Physica D: Nonlinear Phenomena*, 195(1):159–187, 2004.
9. L Billings and EM Bollt. Probability density functions of some skew tent maps. *Chaos, Solitons & Fractals*, 12(2):365–376, 2001.
10. Stefano Boccaletti, Jürgen Kurths, Grigory Osipov, D.L. Valladares, and C.S. Zhou. The synchronization of chaotic systems. *Physics Reports*, 366(1):1–101, 2002.
11. Stefano Boccaletti, Vito Latora, Yamir Moreno, Martin Chavez, and D-U Hwang. Complex networks: Structure and dynamics. *Physics Reports*, 424(4):175–308, 2006.
12. Erik M Bollt and Naratip Santitissadeekorn. *Applied and Computational Measurable Dynamics*. SIAM, 2013.
13. Peter S Bullen, Dragoslav S Mitrinovic, and M Vasic. *Means and their Inequalities*, volume 31. Springer Science & Business Media, 2013.
14. LA Bunimovich, SG Dani, RL Dobrushin, MV Jakobson, IP Kornfeld, NB Maslova, Ya B Pesin, J Smillie, Yu M Sukhov, and AM Vershik. *Dynamical systems, ergodic theory and applications*, volume 100. Springer Science & Business Media, 2000.
15. Scott Camazine, Jean-Louis Deneubourg, Nigel R Franks, James Sneyd, Eric Bonabeau, and Guy Theraulaz. *Self-organization in biological systems*, volume 7. Princeton University Press, 2003.
16. Yongcan Cao, Wenwu Yu, Wei Ren, and Guanrong Chen. An overview of recent progress in the study of distributed multi-agent coordination. *IEEE Transactions on Industrial informatics*, 9(1):427–438, 2013.
17. Maoyin Chen, Yun Shang, Changsong Zhou, Ye Wu, and Jürgen Kurths. Enhanced synchronizability in scale-free networks. *Chaos: An Interdisciplinary Journal of Nonlinear Science*, 19(1):013105, 2009.

18. Pietro De Lellis, Mario di Bernardo, and Franco Garofalo. Synchronization of complex networks through local adaptive coupling. *Chaos: An Interdisciplinary Journal of Nonlinear Science*, 18(3):037110, 2008.
19. Pietro DeLellis, Mario Di Bernardo, and Franco Garofalo. Adaptive pinning control of networks of circuits and systems in lur'e form. *IEEE Transactions on Circuits and Systems I: Regular Papers*, 60(11):3033–3042, 2013.
20. Pietro DeLellis, Mario Di Bernardo, Franco Garofalo, and Maurizio Porfiri. Evolution of complex networks via edge snapping. *IEEE Transactions on Circuits and Systems I: Regular Papers*, 57(8):2132–2143, 2010.
21. Pietro DeLellis, Mario Di Bernardo, Thomas E Gorochowski, and Giovanni Russo. Synchronization and control of complex networks via contraction, adaptation and evolution. *IEEE Circuits and Systems Magazine*, 10(3):64–82, 2010.
22. Sergey N Dorogovtsev and Jose FF Mendes. Evolution of networks. *Advances in Physics*, 51(4):1079–1187, 2002.
23. Yuguang Fang. *Stability analysis of linear control systems with uncertain parameters*. PhD thesis, Case Western Reserve University, 1994.
24. Mattia Frasca, Arturo Buscarino, Alessandro Rizzo, Luigi Fortuna, and Stefano Boccaletti. Synchronization of moving chaotic agents. *Physical Review Letters*, 100(4):044102, 2008.
25. Chris Godsil and Gordon F Royle. *Algebraic graph theory*, volume 207. Springer Science & Business Media, 2013.
26. Olga Golovneva, Russell Jeter, Igor Belykh, and Maurizio Porfiri. Windows of opportunity for synchronization in stochastically coupled maps. *Physica D: Nonlinear Phenomena*, 340:1–13, 2017.
27. Thomas E Gorochowski, Mario Di Bernardo, and Claire S Grierson. Evolving dynamical networks: a formalism for describing complex systems. *Complexity*, 17(3):18–25, 2012.
28. Thomas E Gorochowski, Mario di Bernardo, and Claire S Grierson. Evolving enhanced topologies for the synchronization of dynamical complex networks. *Physical Review E*, 81(5):056212, 2010.
29. Robert Grone and Russell Merris. The laplacian spectrum of a graph ii. *SIAM Journal on Discrete Mathematics*, 7(2):221–229, 1994.
30. Martin Hasler and Igor Belykh. Blinking long-range connections increase the functionality of locally connected networks. *IEICE Transactions on Fundamentals of Electronics, Communications and Computer Sciences*, 88(10):2647–2655, 2005.
31. Martin Hasler, Vladimir Belykh, and Igor Belykh. Dynamics of stochastically blinking systems. part i: Finite time properties. *SIAM Journal on Applied Dynamical Systems*, 12(2):1007–1030, 2013.
32. Martin Hasler, Vladimir Belykh, and Igor Belykh. Dynamics of stochastically blinking systems. part ii: Asymptotic properties. *SIAM Journal on Applied Dynamical Systems*, 12(2):1031–1084, 2013.
33. Martin Hasler and Yuri L Maistrenko. An introduction to the synchronization of chaotic systems: Coupled skew tent maps. *IEEE Transactions on Circuits and Systems I: Fundamental Theory and Applications*, 44(10):856–866, 1997.
34. Boris Hasselblatt and Anatole Katok. *Handbook of dynamical systems*. Elsevier, 2002.
35. Joao P Hespanha and A Stephen Morse. Stability of switched systems with average dwell-time. In *Decision and Control, 1999. Proceedings of the 38th IEEE Conference on*, volume 3, pages 2655–2660. IEEE, 1999.
36. Petter Holme and Jari Saramäki. Temporal networks. *Physics Reports*, 519(3):97–125, 2012.
37. Petter Holme and Jari Saramäki. *Temporal networks*. Springer, 2013.
38. Junji Ito and Kunihiko Kaneko. Spontaneous structure formation in a network of chaotic units with variable connection strengths. *Physical Review Letters*, 88(2):028701, 2001.
39. R. Jeter, M. Porfiri, and I. Belykh. Network synchronization through stochastic broadcasting. *IEEE Control Systems Letters*, 2(1):103–108, Jan 2018.
40. Russell Jeter and Igor Belykh. Synchronization in on-off stochastic networks: windows of opportunity. *IEEE Transactions on Circuits and Systems I: Regular Papers*, 62(5):1260–1269, 2015.

41. Russell Jeter and Igor Belykh. Synchrony in metapopulations with sporadic dispersal. *International Journal of Bifurcation and Chaos*, 25(07):1540002, 2015.
42. Russell Jeter, Maurizio Porfiri, and Igor Belykh. Overcoming network resilience to synchronization through non-fast stochastic broadcasting. *Chaos: An Interdisciplinary Journal of Nonlinear Science*, 28(7):071104, 2018.
43. P. L. Kapitza. Dynamic stability of a pendulum when its point of suspension vibrates. *Soviet Physics JETP*, 21:588–592, 1951.
44. Harold Joseph Kushner. *Introduction to stochastic control*. Holt, Rinehart and Winston New York, 1971.
45. Zoran Levnajić and Igor Mezić. Ergodic theory and visualization. i. mesochronic plots for visualization of ergodic partition and invariant sets. *Chaos: An Interdisciplinary Journal of Nonlinear Science*, 20(3):033114, 2010.
46. Zhi Li and Guanrong Chen. Global synchronization and asymptotic stability of complex dynamical networks. *IEEE Transactions on Circuits and Systems II: Express Briefs*, 53(1):28–33, 2006.
47. Jinhu Lu and Guanrong Chen. A time-varying complex dynamical network model and its controlled synchronization criteria. *IEEE Transactions on Automatic Control*, 50(6):841–846, 2005.
48. Wenlian Lu. Adaptive dynamical networks via neighborhood information: Synchronization and pinning control. *Chaos: An Interdisciplinary Journal of Nonlinear Science*, 17(2):023122, 2007.
49. Naoki Masuda and Petter Holme. *Temporal network epidemiology*. Springer, 2017.
50. Naoki Masuda, Konstantin Klemm, and Víctor M Eguíluz. Temporal networks: slowing down diffusion by long lasting interactions. *Physical Review Letters*, 111(18):188701, 2013.
51. Arghya Mondal, Sudeshna Sinha, and Juergen Kurths. Rapidly switched random links enhance spatiotemporal regularity. *Physical Review E*, 78(6):066209, 2008.
52. Adilson E Motter. Networkcontrology. *Chaos: An Interdisciplinary Journal of Nonlinear Science*, 25(9):097621, 2015.
53. Theoden I Netoff and Steven J Schiff. Decreased neuronal synchronization during experimental seizures. *Journal of Neuroscience*, 22(16):7297–7307, 2002.
54. Takashi Nishikawa and Adilson E Motter. Network synchronization landscape reveals compensatory structures, quantization, and the positive effect of negative interactions. *Proceedings of the National Academy of Sciences*, 107(23):10342–10347, 2010.
55. FWJ Olver, DW Lozier, RF Boisvert, and CW Clark. Nist handbook of mathematical functions, cambridge uni. *Press, Cambridge*, 2010.
56. Edward Ott. *Chaos in dynamical systems*. Cambridge university press, 2002.
57. Louis M Pecora and Thomas L Carroll. Master stability functions for synchronized coupled systems. *Physical Review Letters*, 80(10):2109, 1998.
58. Arkady Pikovsky and Antonio Politi. *Lyapunov exponents: a tool to explore complex dynamics*. Cambridge University Press, 2016.
59. Arkady Pikovsky, Michael Rosenblum, and Jürgen Kurths. *Synchronization: a universal concept in nonlinear sciences*, volume 12. Cambridge University Press, 2003.
60. Maurizio Porfiri. A master stability function for stochastically coupled chaotic maps. *Europhysics Letters*, 96(4):40014, 2011.
61. Maurizio Porfiri. Stochastic synchronization in blinking networks of chaotic maps. *Physical Review E*, 85(5):056114, 2012.
62. Maurizio Porfiri and Igor Belykh. Memory matters in synchronization of stochastically coupled maps. *SIAM Journal on Applied Dynamical Systems*, 16(3):1372–1396, 2017.
63. Maurizio Porfiri and Francesca Fiorilli. Global pulse synchronization of chaotic oscillators through fast-switching: theory and experiments. *Chaos, Solitons & Fractals*, 41(1):245–262, 2009.
64. Maurizio Porfiri and Francesca Fiorilli. Node-to-node pinning control of complex networks. *Chaos: An Interdisciplinary Journal of Nonlinear Science*, 19(1):013122, 2009.
65. Maurizio Porfiri and Francesca Fiorilli. Experiments on node-to-node pinning control of chuas circuits. *Physica D: Nonlinear Phenomena*, 239(8):454–464, 2010.

66. Maurizio Porfiri, Russell Jeter, and Igor Belykh. Windows of opportunity for the stability of jump linear systems: Almost sure versus moment convergence. *Automatica*, 100:323–329, 2019.
67. Maurizio Porfiri and Roberta Pigliacampo. Master-slave global stochastic synchronization of chaotic oscillators. *SIAM Journal on Applied Dynamical Systems*, 7(3):825–842, 2008.
68. Maurizio Porfiri and Daniel J Stilwell. Consensus seeking over random weighted directed graphs. *IEEE Transactions on Automatic Control*, 52(9):1767–1773, 2007.
69. Maurizio Porfiri, Daniel J Stilwell, and Erik M Bollt. Synchronization in random weighted directed networks. *IEEE Transactions on Circuits and Systems I: Regular Papers*, 55(10):3170–3177, 2008.
70. Maurizio Porfiri, Daniel J Stilwell, Erik M Bollt, and Joseph D Skufca. Random talk: Random walk and synchronizability in a moving neighborhood network. *Physica D: Nonlinear Phenomena*, 224(1):102–113, 2006.
71. Wei Ren and Randal W Beard. *Distributed consensus in multi-vehicle cooperative control*. Springer, 2008.
72. Joseph D Skufca and Erik M Bollt. Communication and synchronization in disconnected networks with dynamic topology: Moving neighborhood networks. *Math. Biosci, Eng.(MBE)*, 1(2):347–359, 2004.
73. Paul So, Bernard C Cotton, and Ernest Barreto. Synchronization in interacting populations of heterogeneous oscillators with time-varying coupling. *Chaos: An Interdisciplinary Journal of Nonlinear Science*, 18(3):037114, 2008.
74. Francesco Sorrentino and Edward Ott. Adaptive synchronization of dynamics on evolving complex networks. *Physical Review Letters*, 100(11):114101, 2008.
75. Andrzej Stefański, Przemyslaw Perlikowski, and Tomasz Kapitaniak. Ragged synchronizability of coupled oscillators. *Physical Review E*, 75(1):016210, 2007.
76. Toni Stojanovski, Ljupco Kocarev, Ulrich Parlitz, and Richard Harris. Sporadic driving of dynamical systems. *Physical Review E*, 55(4):4035, 1997.
77. David J.T. Sumpter. *Collective Animal Behavior*. Princeton University Press, Princeton, NJ, 2010.
78. Yang Tang, Feng Qian, Huijun Gao, and Jürgen Kurths. Synchronization in complex networks and its application–a survey of recent advances and challenges. *Annual Reviews in Control*, 38(2):184–198, 2014.
79. Wenwu Yu, Pietro DeLellis, Guanrong Chen, Mario Di Bernardo, and Jürgen Kurths. Distributed adaptive control of synchronization in complex networks. *IEEE Transactions on Automatic Control*, 57(8):2153–2158, 2012.
80. Damián H Zanette and Alexander S Mikhailov. Dynamical systems with time-dependent coupling: clustering and critical behaviour. *Physica D: Nonlinear Phenomena*, 194(3):203–218, 2004.